Rationally design of a proline transporter inhibitor with anti-*Trypanosoma cruzi* activity.

Lucía Fargnoli[1], Esteban A. Panozzo-Zénere[1], Lucas Pagura[3], María Julia Barisón[2], Julia A. Cricco[3], Ariel M. Silber[2] and Guillermo R. Labadie[1,*]

[1]Instituto de Química de Rosario (IQUIR), Facultad de Ciencias Bioquímicas y Farmacéuticas. Universidad Nacional de Rosario. Rosario, Argentina.

[2]Laboratory of Biochemistry of Tryps-LaBTryps, Departamento de Parasitologia, Instituto de Ciências Biomédicas, Universidade de São Paulo, Av. Lineu Prestes 1374, Cidade Universitária, São Paulo, Brazil.

[3]Instituto de Biología Molecular y Celular de Rosario (IBR), Consejo Nacional de Investigaciones Científicas y Técnicas CONICET–Facultad de Ciencias Bioquímicas y Farmacéuticas, Universidad Nacional de Rosario, Rosario, Argentina.

Corresponding author: labadie@iquir-conicet.gov.ar

Tel.: +54-341-4370477 # 108

Fax: +54-341-4370477 # 112

Highlights

A rationally design L-proline transporter inhibitor have been proposed.

Sixteen compounds were prepared and tested on *T. cruzi* epimastigotes.

Inhibition of L-proline uptake was validated and linked to the antichagasic activity.

A fluorescent analog was synthesized for localization and internalization studies.

Fluorescent microscopy showed the analog distributed along the parasite cytoplasm.

Abstract

L-Proline is an important amino acid for the pathogenic protists belonging to *Trypanosoma* and *Leishmania* genera. In *Trypanosoma cruzi*, the etiological agent of Chagas disease, this amino acid is involved in fundamental biological processes such as ATP production, differentiation of the insect and intracellular stages, the host cell infection and the resistance to a variety of stresses, including nutritional and osmotic as well as oxidative imbalance. In this study, we explore the L-Proline uptake as a chemotherapeutic target for *T. cruzi*. For this, we propose a novel rational to design inhibitors containing this amino acid as a recognizable motif. This rational consists of conjugating the amino acid (proline in this case) to a linker and a variable region able to block the transporter. We obtained a series of sixteen 1,2,3-triazolyl-proline derivatives through alkylation and copper(I)-catalyzed azide-alkyne cycloaddition (click chemistry) for *in vitro* screening against *T. cruzi* epimastigotes, trypanocidal activity and proline uptake. We successfully obtained inhibitors that are able to interfere with the amino acid uptake, which validated the first example of a rationally designed chemotherapeutic agent targeting a metabolite's transport. Additionally, we designed and prepared fluorescent analogues of the inhibitors that were successfully taken up by *T. cruzi*, allowing following up their intracellular fate. In conclusion, we successfully designed and produced a series of metabolite uptake inhibitors. This is one of few examples of rationally designed amino acid transporter inhibitor, being the first case where the strategy is applied on the development of chemotherapy against Chagas disease. This unprecedented development is remarkable having in mind that only a small percent of the metabolite transporters has been studied at the structural and/or molecular level.

Keywords: Chagas disease; Proline uptake; fluorescence microscopy; *T. cruzi* epimastigotes; citotoxicity; target validation.

.

1. Introduction

Chagas disease is one of the most neglected infectious diseases. It is endemic in the Americas, having 8-10 million people infected with 25 million people at risk. With the increment of travelers and migration waves, a growing presence of imported cases in Europe, USA, Canada, and Japan has occurred and increase potential for local transmission through non-vectorial routes.[1] The disease is classically divided in two phases: acute and chronic. The acute phase is characterized by a noticeable parasitemia and the absence of humoral response. It is largely asymptomatic, and it may present unspecific symptoms making it difficult to diagnose. The chronic phase is characterized by a non-evident parasitemia and a robust IgG response and is asymptomatic in 60-70% of the cases (indeterminate form). The main clinic forms, when present, are the cardiac or cardio-digestive with specific symptoms.[2] The chemotherapy against Chagas disease relies mainly on two drugs introduced more than 40 years ago: Nifurtimox (Nf) and Benzonidazole (Bz).[3] Both drugs are efficient for treating the acute phase, but their use in the chronic phase, when most of patients are diagnosed, is controversial. In addition, severe side effects due to toxicity and, more recently, the emergence of resistance have been reported, increasing the urgency to develop new chemotherapies.[4]

Trypanosoma cruzi is a hemoflagellated parasite that causes Chagas disease. This parasite presents a complex life cycle among two kinds of hosts: mammals and reduviid insects, which transmit the infection. Along its life-cycle at least four stages were clearly identified, epimastigotes (replicative stage) and metacyclic trypomastigotes (infective, non-replicative stage) in the insect and blood stream trypomastigotes and amastigotes (intracellular replicative stage). Also, during its life-cycle the parasite faces different environments and it

must adjust its “life-style” including its metabolism to changes in nutrients availability, temperature, among other environmental variables.

Among many other important metabolites, amino acids are particularly relevant for the biology of *T. cruzi* beyond their obvious participation in protein synthesis,[5] playing fundamental roles in energy management[6] and nitrogen metabolism.[7, 8] When epimastigotes proliferation arrests, there is a metabolic switch from a carbohydrates to an amino acids based metabolism, with a consequent change in the protein expression profile.[9, 10] In fact, it has been demonstrated that amino acids such as proline,[11] histidine,[12] and even alanine,[8] as well as the proline oxidation product P5C,[13] can fuel electrons to the respiratory chain, powering the mitochondrial ATP synthesis.[11, 12, 14, 15] Some neutral amino acids can also function as osmolytes, serving to counteract volume perturbations following a shift in extracellular osmolarity.[9, 16, 17] These functions results crucial when the parasite moves from one environment to another, helping the adaptation process.[5]

Particularly, proline is involved in several of the mentioned processes, such as the energization of the host-cells invasion by metacyclic trypomastigotes,[15] as well as growth and differentiation of the insect[18-20] and the intracellular stages.[19] Additionally, its accumulation in the parasite cytoplasm provides resistance to oxidative and thermal stress.[11, 19, 21, 22] The proline availability is mediated by an interplay of the biosynthesis degradation and uptake process. [11, 14, 21-24] In particular, the inhibition of proline uptake by competitive transporter interrupters, diminished the parasites ability to tolerate oxidative imbalance, nutritional stress and to complete the infection cycle.[21]

Taking the proline uptake as a novel drug target we decided to develop new transporter inhibitors and evaluate their antiproliferative activity. These new compounds were initially

evaluated on *T. cruzi* epimastigotes, validating their action mechanism by proline transport experiments. A comprehensive analysis of the structure-activity relationship allowed a rational pipeline to design selective metabolite transporter inhibitors. Finally, we designed and synthetized a fluorescent analog, which allowed us to visualize the subcellular fate of this compound in *T.* cruzi epimastigotes.

2. Results and discussion

2.1 Design of Proline transport inhibitors

The selective inhibition of transporters has been proposed as a valuable target to develop new medications. The interruption of lipid, sugar and amino acid trafficking has been studied looking for the treatment of diverse pathologies. Serotonin and norepinephrine reuptake inhibitor have been appointed as possible antidepressants.[25, 26] GABA transporter inhibitors seem particularly attractive as anticonvulsant drugs.[27] The endogenous cannabinoid system is considered an important therapeutic target for the treatment of diverse pathologies, including asthma, pain, multiple sclerosis, malignant gliomas, and neurodegenerative diseases. The selective inhibition of the endocannabinoid uptake has been studied[28, 29] for the potential therapeutic value in the treatment of disorders characterized by a low endocannabinoid activity, like Huntington's chorea or multiple sclerosis.

A remarkable example of that approach has been the development of Ezetimibe®, a novel cholesterol-lowering agent.[30] This compound was initially found in a CAT (acylcoenzyme A cholesterol acyltransferase) inhibitors' campaign. Many years of extensive investigation supports the notion that NPC1L1 (Niemann–Pick C1-Like 1, an intestinal cholesterol transporter), is the molecular target of Ezetimibe.[31] This serendipitous discovery ended up being a successful case of a metabolite transporter as a validated target of a drug.

The specific inhibition of neuronal glycine, alanine, serine, and cysteine transporters have been studied as molecular targets for new treatment of schizophrenia.[32] In particular, an inhibitor of glycine transporter GlyT2 has been studied as a potential treatment for schizophrenia and alleviation of pain.[33] RG1678, a novel compound from Roche, is one of the most advanced GlyT1 inhibitors, selective toward GlyT2 that went into clinical trials.[34] A high-affinity transporter for proline has been identified, providing an important evidence for proline as a neurotransmitter.[35] A high throughput screening campaign for high affinity proline transporter inhibitors, with a library of approximately 300,000 compounds, resulted in the identification of the selective inhibitor LP-403812.[36]

Summarizing, the participation of metabolites uptake in critical processes in health and diseases has been well demonstrated. However, a systematic rational design pipeline for molecules targeting molecular transporters has not been properly exploded. Therefore, the discovery of most of transporters inhibitors happened by chance or through large HTS campaigns. Burns *et al.*[37] pioneered a work in this sense proposing a polyamine-fatty acid conjugate as a polyamine transporter inhibitor. In their rational, the polyamine portion is recognized by the transporter and the fatty acid interacts with the membrane, blocking the polyamine entrance. The newly designed inhibitors (L-Lyz(C18-Acyl-spermine) combined with DMFO display selective antitumoral activity. All the inhibitors mentioned before contained an amino acid portion, or an amino acid mimic, that is recognized by the transporter as a common feature. (**Figure 1**)

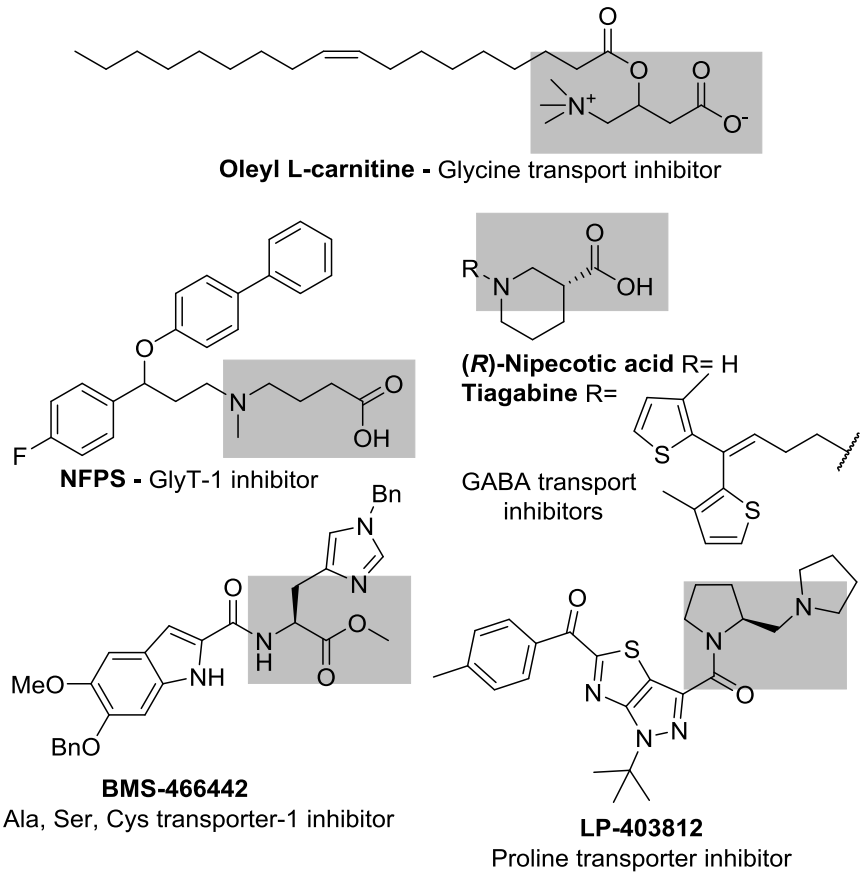

Figure 1. Known amino acid transport inhibitors.

With those precedents in mind, we established the basis for the design of new amino acid transport inhibitor. A proper uptake blocker needs to be recognized by the transporter, but not being able to go through, by adding a bulky substituent or a membrane interacting portion that prevents its transport. (**Figure 2**)

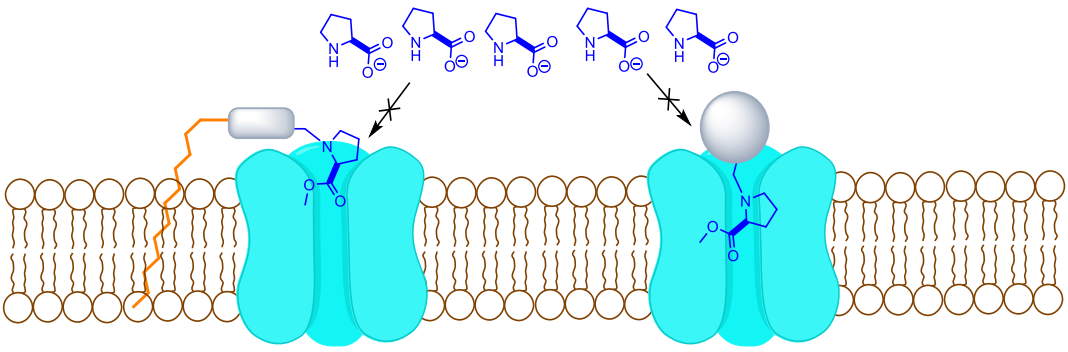

Figure 2. Proposed model for transport inhibition.

This model will require a compound holding a recognition motif, a linker and a membrane anchor or a voluminous substituent to block the L-proline incorporation. The recognition portion will have L-proline to specifically interact with the transporter, the membrane anchor should be a non-polar group and both parts will be connected by a 1,2,3-triazole. (**Figure 3**)

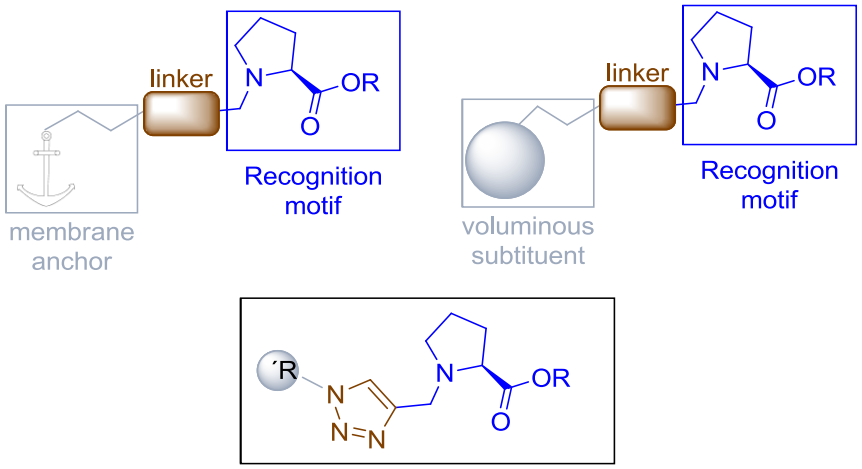

Figure 3. Rational design of proline transport inhibitors.

The outcome of click chemistry had a strong impact in many research areas including Medicinal Chemistry.[38, 39] The easy access to a collection of compounds has made this methodology very useful to rapidly prepare collections of compounds, being also applied on antiparasitic drug discovery.[40-42] The neutral nature of the 1,2,3-triazole formed in this

reaction have properly suited the requirements for bioconjugation, protein labeling and immobilization[43, 44] and for combining different pharmacophores to make hybrid compounds or chimeras. Using 1,2,3-triazole as linkers the product should require substituents with proper membrane anchor properties. Fatty acids and isoprenyl chains are selectively introduced in proteins by post translational modifications and serves as a mediator for membrane association increasing their molecular hydrophobicity.[45] Looking to produce a similar anchoring properties, isoprenyl and linear long alkyl chain were selected as some of the triazole substituents, introduced as azide on the heterocycle. Additionally, looking to block the transporter, azides with bulky substituent were also included.

2.2. Synthesis

To validate the proposed model, we proceeded to make a small library following the synthetic strategy shown on **Scheme 1**. The synthesis started from commercial L-proline, preparing the key intermediate in two steps, including an esterification to produce the methyl prolinate **1** followed by an N-alkylation with propargyl bromide. Once the required key propargyl methyl prolinate **2** intermediate was prepared, a pool of different azides covering a variety of steric moieties including, aryl, alkyl and isoprenyl substituents was proposed to explore their capacity to interact with the membrane. Azides were prepared by direct substitution of bromide with sodium azide on DMF except for geranyl-,farnesyl-, and phytylazides, which were synthesized from geraniol, farnesol and phytol respectively using diphenylphosphorylazide (DPPA) following Thompson's procedure.[46] Phytylazide was found to be a mixture of three chemical entities in equilibrium: tertiary azide, *E* and *Z* isomers of the primary azide, following the same behavior previously observed on geranyl-and farnesylazide.[40] Allylic azides can be obtained as a mixture, because they exist as

equilibrating mixtures of regioisomers due to the [3,3] sigmatropic rearrangement (Winstein rearrangement).[47] That was the case of geranyl, farnesyl and phytylazide, a mixture of primary:tertiary (8:1), being the primary as 1.6:1 (*E*:*Z*) ratio.[48]

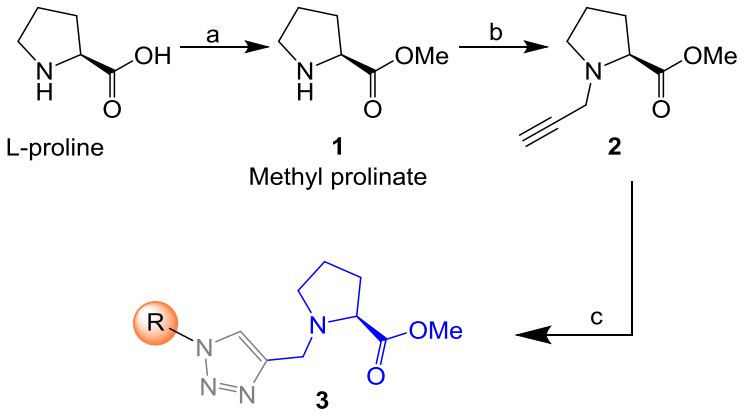

a) HCl/Methanol, R.T., 6 h; b) propargyl bromide, NEt_3, Et_2O;
c) R-Azide, t-butanol: H_2O (1:1), sodium ascorbate, $CuSO_4$ 1 M.

Scheme 1. Synthesis of proline transport inhibitors.

Having prepared the pool of azides, we continued with the preparation of a focused library of inhibitors through click chemistry. Reactions were conducted in a parallel solution synthesis setup under copper (II) sulphate catalytic conditions in water:*t*-BuOH (1:1), using sodium ascorbate as a reductant.[49-51] In general, reactions needed an excess of azides for completion and a reaction time was 18 h. All the products have 1,4-substitution on the 1,2,3,-triazol as expected, based on the original description of this methodology and our previous work.[40, 50] Reactions with aliphatic and benzylic azides produced a single product, with yields that are slightly better for the last ones. The reaction with the mixture of geranyl azides generated **3i,** which was identified as an inseparable mixture of *E* and *Z* isomers (^{1}H NMR, 1.5:1), in accordance with our previous results.[40] When farnesyl azide was used, a mixture of regioisomers was also obtained with the same ratio, but in this case they were separable.

(**Figure 4)** When phytylazide was used the same regioisomers were isolated after the reaction with N-propargyl methyl prolinate **1**, presenting a higher *E*:*Z* ratio (1.8:1). Extensive purification work allowed only the isolation of the *E*-isomer of a pure compound (**3p-*E*, Figure 4**), leaving the remaining product **3q** as a mixture *E*:*Z*.

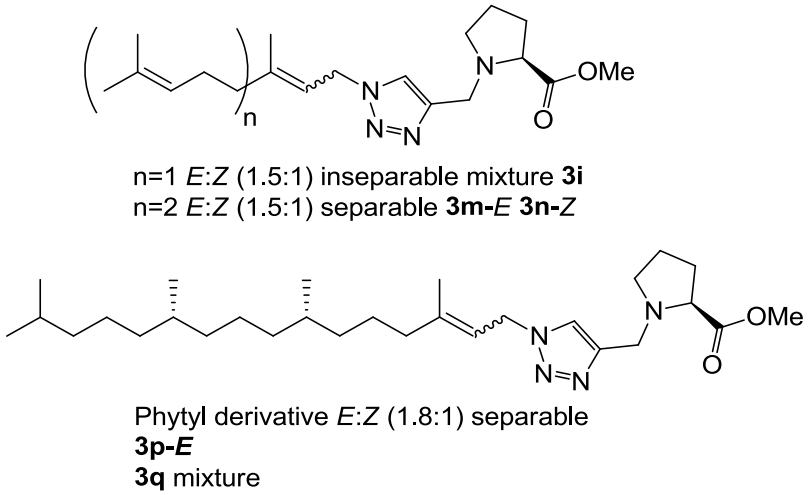

Figure 4. Prenyl analogs prepared.

Final products **3a-3q**, presented in **Table 1,** were obtained with an average 67 % yield after purification and were completely characterized by 1D and 2D NMR and ESI-HRMS.

2.3. Biological evaluation

In order to evaluate the biological activity of the prepared collection we decided to initially determine the activity on *T. cruzi* insect forms (epimastigotes). Then, to validate the L-proline transporter as the molecular target, the intracellular concentration of the amino acid was measured in competition assays with compounds that shown the best antiparasite activity. Finally, the cytotoxicity of the selected candidates was evaluated in African green monkey kidney epithelial (VERO) cells to estimate the selectivity toward the parasite.

2.3.1. *In vitro* activity against *T. cruzi* epimastigotes

The compounds collection was assayed against *T. cruzi* epimastigotes (CL strain clone 14)[52] at a maximum concentration of 100 μM. Eight of the compounds did not show activity at that concentration (**3a**, **3b**, **3c**, **3d**, **3e**, **3f**, **3h**, **3m**). A detailed analysis of the activities revealed that compounds **3a** and **3b** are considerable shorter than the rest of the library and have esters on the side-chain. Being the most polar substituent of the series and susceptible of hydrolysis a possible reason for their lack of activity. Analogs **3c**, **3d**, **3e** and **3f** contain cyclic substituents, both arylic and alicyclic. The naphtyl derivative **3g**, the bulkier members or the collection, has an IC_{50} of 100 μM, implying that polycyclic substituents could be required to improve the activity. Nevertheless, the fact that the aromatic analogs were inactive discouraged the idea that π-stacking interaction would contribute to increase the binding affinity to the molecular target.

Table 1. Anti-*T. cruzi* activity of the proline derivatives.

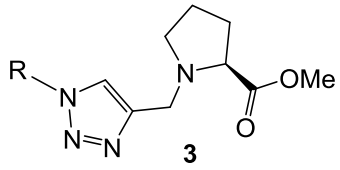

3

Compound	R	Yield %	*T. cruzi*[a] IC_{50} [μM]
3a	CH_2COOEt	80	> 100
3b	$(CH_2)_4COOEt$	69	> 100
3c	Bn	80	> 100
3d	Cyclohexyl	39	> 100
3e	Ph-$CH_2CH_2CH_2$	82	> 100
3f	Cinnamyl	60	> 100
3g	CH_2-naphtyl	81	100
3h	Octyl	81	> 100
3i	Decyl	75	38.00
3j	Cetyl	42	24.54
3k	Oleyl	59	39.98
3l	Eicosanyl	58	100
3m	Geranyl	87	> 100
3n	*E*-Farnesyl	43	48.93
3o	*Z*-Farnesyl	23	59.39
3p	*E*-Phytyl	38	67.81
3q	Phytyl-Mixture	39	44.16
Benznidazole			7.0[53]

a) Epimastigotes CL14

As mentioned before, fatty acids and isoprenyl chains contribute as mediators for protein membrane anchoring, being the reason why 10 analogs were included with those substituents. In general terms, the hypothesis that this kind of substituents contribute to improve the activity seems to be validated because only the analogs holding the shorter substituents, **3h** (R=octyl) and **3m** (R=geranyl) were inactive. A detailed look at the aliphatic derivatives' activities did not show a direct correlation between the IC_{50} and the chain length. The activity increases from octyl **3i** to decyl **3h** derivative (IC_{50}>100 and 38.00 μM, respectively), being the cetyl analog **3j**, with an IC_{50} 24.54 μM, the most active. Then, the activity decreases to 39.98 μM for the oleyl derivative **3k** and 100 μM for the eicosanyl analog **3l**. A similar behavior is observed for the prenyl derivatives, but in this case the difference is less pronounced. Moving from the geranyl derivative **3h** to the farnesyl analogs the activity increase to 48.93 μM for the *E*-isomer **3n** that is slightly more active than the *Z*-isomer **3o** (59.39 μM). Then, as happened with the alkylated analogs, the activity decreases for the longer member of the family, the phytyl derivatives **3p** (*E*-isomer) and **3q** (E/Z mixture), with IC_{50}s 67.81 and 44.16 μM respectively.

That behavior can be clearly seen on the log IC_{50}/carbon chain plotted, where the aliphatic and the prenylated have been correlated separately. (**Figure 5**) One interesting output of this chart is that both curves have their minimum around 13 carbon atoms, that appears to be the optimal chain length.

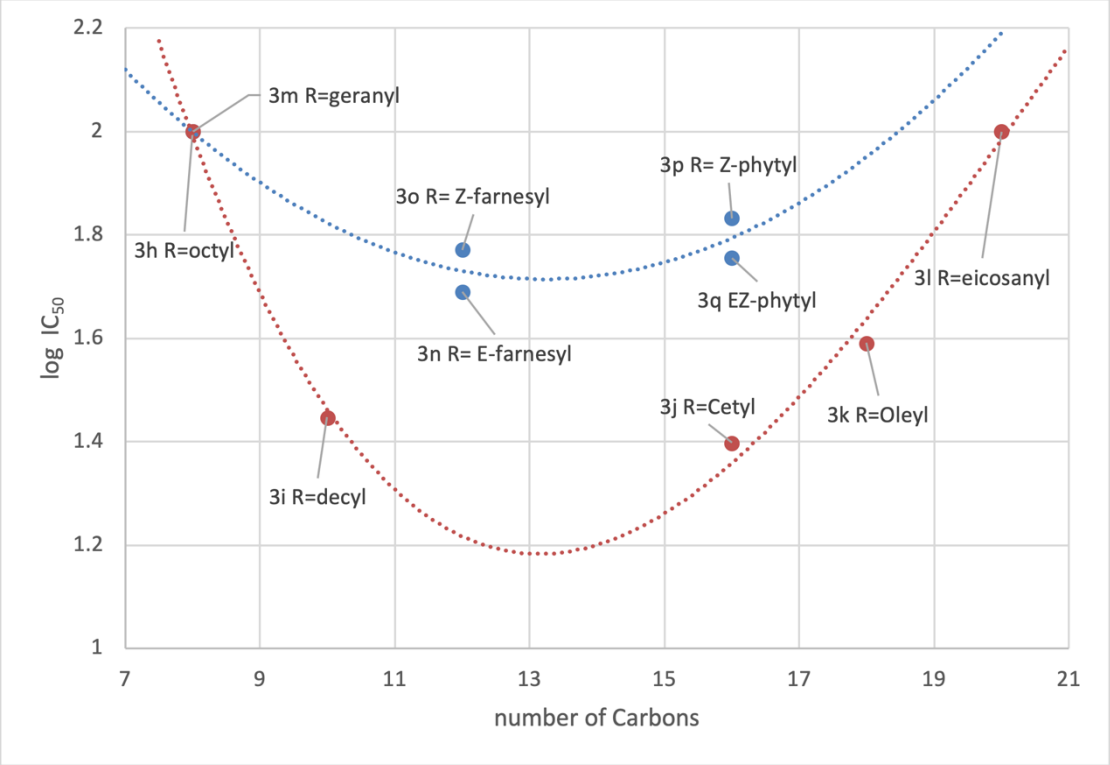

Figure 5. Correlation between activity and substituents chain length. (blue: prenyl, red: aliphatic)

A comparison of the most active compounds have shown that are considerable more active than L-thiazolidine-4-carboxylic acid (T4C), the only reported antichagasic proline derivative, with an IC_{50} of 890 μM on *T. cruzi* epimastigotes.[21] Analogs **3j**, **3i**, **3k**, **3n** were 36, 23, 22, and 18 times more active than the thiazolidine proline analog. That marked difference on the activity highlight the importance of the proline ring decoration on the antiparasitic activity.

2.3.2. *In vitro* cytotoxicity assay on Vero cells.

Vero cells are well established model to test cytotoxicity *in vitro* because is an aneuploid and a continuous cell linage. Initially the library was screened at a fix concentration of 4.75

μg/mL and none of the analogs showed cytotoxic activity. The most active analogs of the series compounds **3i**, **3j**, **3k**, and **3n** were submitted to a further analysis to determine their IC_{50}. Compound **3j** was not soluble at 50 μM which made not possible to calculate its IC_{50}. Analogs **3i**, **3k**, and **3n** were soluble in a concentration range allowing to perform the assay, showing IC_{50} of 43 μM, 17 μM and 14 μM, respectively. Those values established the adequate concentration window for future studies of those analogs on *T. cruzi* intracellular stages. The selectivity index, (calculated as IC_{50}Vero cells / IC_{50} *T. cruzi* epimastigotes) were 1.13, 0.43 and 0.25 for compounds **3i**, **3k**, and **3n**, respectively. This numbers shown a similar susceptibility to the compounds. The toxicity displayed may be linked to the proline transport inhibition.

2.3.3. Proline transport assay.

In order to obtain a deeper insight into the molecular mechanism of the most active compounds, we performed a proline transport competition assay. The compounds with an IC_{50} lower than 50 μM (**3i**, **3j**, **3k**, **3l** and **3n**) were selected to perform the proline uptake assay aiming to determine the transport inhibition.[21] The analogs were assayed on *T. cruzi* epimastigotes incubated with proline at the transporter Km concentration (0.31 mM),[24] were the analogs were assayed a concentration 10-fold higher (3.1 mM). Surprisingly, we observed that the compounds with higher activity on *T. cruzi* epimastigotes (lower IC_{50} values) showed inhibition but were not strong enough when compared to analogs with lower antiparasitic activity (higher IC_{50} values**).** As can be seen on **Figure 6,** compounds **3i** (*T. cruzi* epimastigotes IC_{50}=38 μM) and **3n** (*T. cruzi* epimastigotes IC_{50}=49 μM) showed a proline transport inhibition higher than 75% being more active than the analog **3j** that only reduce the inhibition in 20%. The oleyl derivate (**3k**), with an unsaturated fatty tail, has a

similar IC_{50} on *T. cruzi* epimastigotes compared to the cetyl analog (**3j**) showing no inhibition in terms of proline uptake. (**Table 2**)

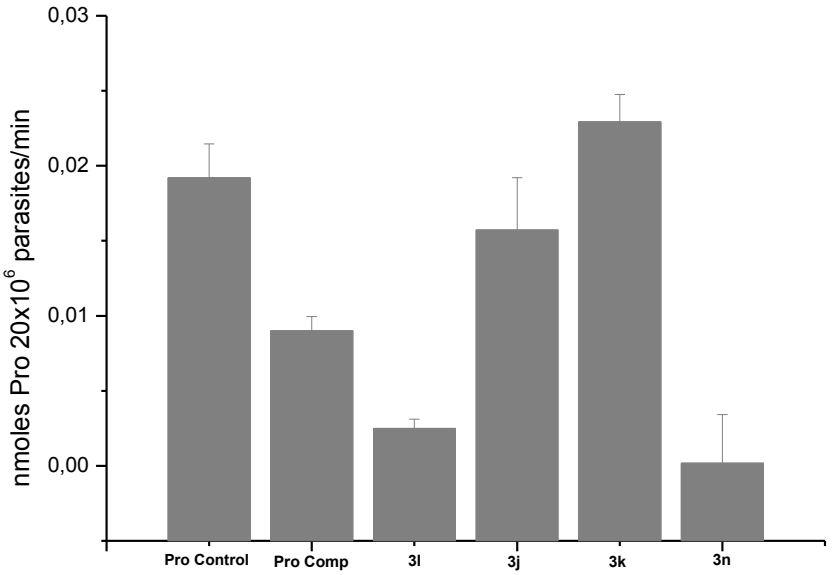

Figure 6. Proline uptake assay. Pro control = Proline control, Pro comp = L-Proline as competitor. **3i-k** and **3n** = proline analogs level incubated with selected analogs. Pro control (0.31 mM L-proline, [^{3}H] proline, PBS). Pro Comp (3.1 mM L-proline, [^{3}H] proline, PBS). Compounds **3i-k** and **3n** (0.31 mM L-proline, 3.1 mM analog **3x**, [^{3}H] proline, PBS). Stop solution: 50 mM L-proline added after 30 seconds.

The first hypothesis to explain that behavior was based on the unsaturation of the side-chain that has a twisted conformation produced by the C9–double bond that also restricts the rotation around the neighbor bonds. As we could observe by comparison of the structure of compounds **3i** and **3j**, the differences relay on the unsaturation of the carbon tail.

Furthermore, the tail length of **3i** and **3j** differ in 6 carbon and the most active is the decyl analogue (**3i**) in terms of transport inhibition, matching the behavior displayed in **Figure 5**.

Table 2. Proline uptake inhibition of selected analogs.

Compound	R	*T. cruzi*	% of Proline inh.
3i	Decyl	38.22	87
3j	Cetyl	24.54	18
3k	Oleyl	39.98	0
3n	*E*-Farnesyl	48.93	99

The remaining tested analog, the *E*-farnesyl derivative **3n,** is an isoprenyl derivative, with a trimethyl substituted side-chain that is twelve carbon long, with three double bonds. Interestingly, this analog produced a complete inhibition of the proline uptake but is the less active of this series against *T. cruzi*. (**Table 2**) The fact that this analog was a better inhibitor of the transporter could be the result of a better binding. Also, could be attributed to the markedly different conformation of the analog due to the restricted rotation of the isoprenyl chain. Those restrictions should contribute to block the transporter once the proline region is recognized.[54]

Comparing the inhibition of proline uptake by T4C, the analogs **3i** and **3n** resulted considerably more active.[21] Those differences were clearly related with the N1-alylated-1,2,3-triazolyl chain introduced on the proline.

2.3.4. Proline analog internalization

In order to evaluate the possible incorporation of L-proline analogs, we designed and synthesized a fluorescent proline analog, with a structure that preserved the structural requirements who will contribute to the **3i** activity (R=decyl).

To prepare a fluorescent analogs of bioactive compounds there are two strategies. One of them, requires the incorporation of the marker into the native molecule by covalent binding through existing functional groups. That is a valid approach, but due to the increment of the size, shape and the polarity of the target molecule, the action mechanism can be altered. Alternatively, the fluorescent derivative can be prepared by exchanging a portion of target molecule for a modified fluorophore. The first strategy is commonly used with natural products and complex molecules; and the second one is applied on synthetic compounds, in particular for those that require short reaction routes.[55] In our case, based on the lack of a easily derivatizable group, the second strategy was chosen. The analog **3i** was selected as a template because it has a good antiparasitic and transport inhibitor activity, being more accessible synthetically because contains just an alkyl chain on the 1,2,3-triazol. The proposed fluorescent derivative incorporated a 7-Amino-4-nitro-2,1,3-benzoxadiazole group (amino NBD) as fluorophore at the end the decyl chain. (**Figure 7**) NBD was selected as fluorophore because it has been extensively used as a fluorescent reporter of many metabolites including cholesterol,[56] phospholids,[57] fatty acids[58] and for natural products.[59] To estimate how the design fluorescent analog mimic of **3i** the most important topological descriptors were calculated. Using molinspiration platform[60] logP and TPSA were calculated showing small differences on both parameters. LogP was very similar for both (**3i** =4.62, **3i-NBD** =5.03), the topological polar surface area (TPSA) was considerable higher for **3i-NBD** (**3i** =60.26 vs **3i-NBD**=157.04) and the volume was bigger for the

fluorescent analog as was expected (**3i** = 359.38, **3i-NBD** = 484.01). Besides the differences on the volume and the TPSA, that are consequence of the NBD located on the aliphatic tail, did not considerably affect the logP being therefore a good model.

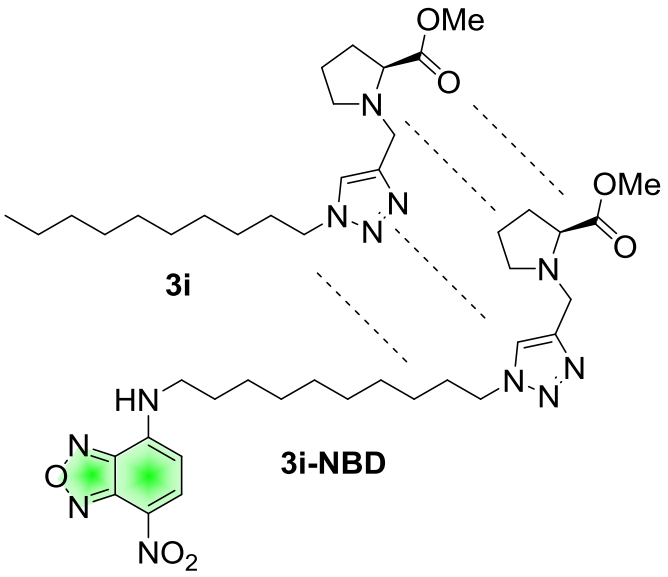

Figure 7. Similarities between 3i and 3i-NBD. The fluorescent analog preserves the most important portion of **3i**.

3i-NBD could be prepared by CuAAC of the intermediate **1** and the N-NBD-10-azidodecan-1-amine (NBD-azide). The necessary NBD-azide was prepared in 3 steps stating from 1,10-dibromodecane. The dibromo was converted to the corresponding 1,10-diazidodecane **5** by direct substitution with sodium azide,[61] and then selectively reduced to the amino-azide **6** with triphenylphosphine in a biphasic system.[62] (**Scheme 2**) Finally, the fluorophore was incorporated by electrophilic aromatic substitution of the NBD-Cl using cesium carbonate as base to afford the expected NBD-azide product **7**.[63] Then, by CuAAC following the previously mentioned procedure the final NDB derivative **3i-NBD** was obtained.(**Scheme 2**)

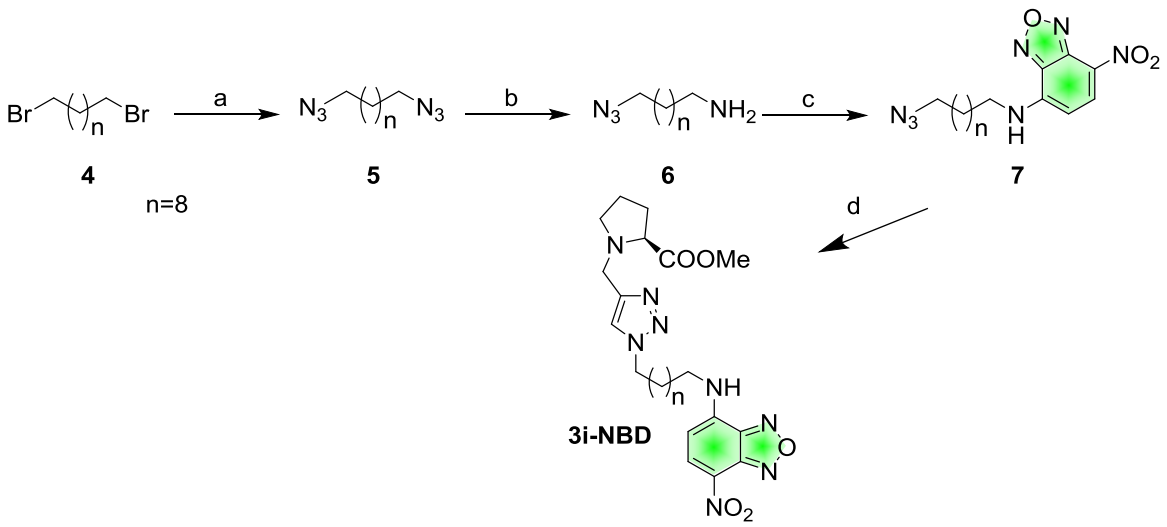

Scheme 2.a) NaN_3, DMF, 40 °C, 76%; **b)** PPh_3, DCM-ac 0.65M H_3PO_4, RT, 12%; **c)** NBD-Cl, Cs_2CO_3, THF, 50 °C, 31%; d) **2**, t-BuOH:H_2O (1:1), 1M sodium ascorbate, 1M $CuSO_4$, RT, 58%.

First, the spectroscopic profile of the **3i-NBD** was studied. The UV-vis and fluorescent spectra were acquired, and the maximum of excitation and emission fluorescence were determined, being 472 nm and 538 nm respectively.[64] (See supporting information) To analyze the incorporation of **3i-NBD** in epimastigotes we incubated them with different concentrations of this analog (10 μM, 25 μM and 30 μM) during 30 min. Then, the samples were washed and treated to their evaluation by confocal microscopy similarly to the studies reported by Merli *et al*.[65] In this study, the better images were obtained when epimastigotes were incubated with 25 μM of **3i-NB,** and they are shown in **Figure 8**.

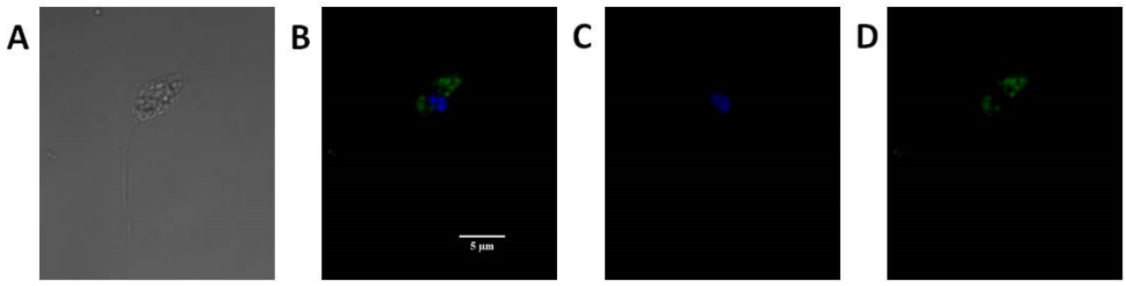

Figure 8. Localization of **3i-NBD** in *T. cruzi*. Epimastigotes were incubated during 30 min, at 28°C with 25 μM **3i-NBD**. Incorporation was evaluated by confocal microscopy. Panel (A) shows the parasite using differential interference contrast (DIC) microscopy. Panel (B) shows intracellular distribution of **3i-NBD** following incubation with DAPI and **3i-NBD**. Panel (C) show the results of labeling with DAPI (blue). Panel (D) show the results of labeling with **3i-NBD** (green). The results are representative of at least three independent experiments.

The analysis of obtained confocal images clearly showed that the green fluorescent signal of **3i-NBD** was punctually localized in the parasite cytoplasm and excluded from the plasmatic membrane. This result confirms that this compound was internalized by epimastigotes, suggesting that **3i-NBD** could compete with proline for its specific transporter. It has previously reported that the analog **3i** was not as effective as **3n** as proline transport inhibitors.[54] Indeed, the transport inhibition differences were justified on the restricted conformation of **3n** due to the multiple double bonds of the farnesyl chain. Additionally, the experiment on the transgenic parasites that overexpresses the TcAAAP069 proline permease shown that parasites treated with the compound **3n** did not incorporate proline after 1 h incubation.[54] That result suggested that this compound could probably be an irreversible

inhibitor of the permease. The fact that the fluorescent analog **3i-NBD** was able to be internalized through the parasite cytoplasm implied that has a different inhibition mechanism that **3n**, probably competing with proline and other metabolites. That could also apply for the cetyl derivative **3j** that was the most active analog but a poor transport inhibitor. On the other hand, the pattern of the fluorescent signal of **3i-NBD** suggested that this compound could be accumulated in internal vesicles, indicating that the natural path of the transported proline occurs via these vesicles or that aliphatic tail anchor the compound to any membrane system. Proline uptake has been studied using the tritium labelled amino acid. The fact that **3i-NBD** could be internalized by a transporter open up the opportunity to design new fluorescent analogs to study amino acids transport.

3. Conclusions

In the present study a strategy to rationally design amino acids transport inhibitors was proposed. The uptake blocker is composed by a recognition motif, a linker and a bulky substituent or a membrane interacting portion. A set of seventeen 1,5-subtituted-1,2,3-triazole derivatives of methyl prolinate were prepared to validate the design. They were initially assayed against *T. cruzi* epimastigotes showing comparable potency than the control drug benznidazole. The trypanocidal activity profile of the series allowed us to establish a well-defined structural-activity relationship were the nature of the side-chain play a critical role. In order to validate the design, the inhibition of the proline uptake was studied with the analogs **3i**, **3j**, **3k**, **3l** and **3n** that displayed the best antiparasitic activity. The analogs with **3i** (R=decyl) and **3n** (R=*E*-farnesyl) produced a markedly reduction of the proline internalization. Those studies are strong evidence to validate our design of the transported

inhibitor that also linked the antiparasitic activity with the proline uptake. Additionally, the compound **3i** was tagged with NBD to make a fluorescent analog to track the compound uptake. That strategy remains almost unexplored for antiparasitic drugs action mechanism studies, with few exception including miltefosine,[66] artemisinin[67] and chloroquine.[68]

The green fluorescent signal of the NBD derivative of compound **3i** was localized in the parasite cytoplasm. These findings suggest that the compound was internalization and was not bound to the membrane permease. This result, together with the proline uptake inhibition, allowed us to postulate that **3i** could be competing with the amino acid incorporation.

Besides the promising application of the design strategy and the proline inhibitor, the newly prepared compounds are not selective enough to be considered as antichagasic drug candidates. Nevertheless, further studies on the other *T. cruzi* life cycle stages could confirm or discard that hypothesis.

4. Materials and methods

4.1. General

Chemical reagents were purchased from commercial suppliers and used without further purification, unless otherwise noted. Dry, deoxygenated diethyl ether (Et_2O), tetrahydrofuran (THF), and dichloromethane (DCM) were obtained bypassing commercially available pre-dried, oxygen-free formulations through activated alumina columns. DMF was distilled from BaO. Reactions were monitored by thin-layer chromatography (TLC) performed on 0.2 mm Merck silica gel aluminum plates (60F-254) and visualized using ultraviolet light (254 nm) and by potassium permanganate and heat as developing reagents. All reactions were performed under an atmosphere of nitrogen using oven-dried glassware and standard

syringe/septa techniques. Column chromatography was performed with silica gel 60 (230-400 mesh). Yields were calculated for material judged homogeneous by thin layer chromatography (TLC) and nuclear magnetic resonance (^{1}H NMR).

^{1}H and ^{13}C NMR spectra were acquired on a Bruker Avance II 300 MHz (75.13 MHz) using $CDCl_3$ as solvent. Chemical shifts (δ) were reported in ppm downfield from tetramethylsilane and coupling constants are in hertz (Hz). NMR spectra were obtained at 298 K unless otherwise stated and samples run as a dilute solution of the stated solvent. All NMR spectra were referenced to the residual undeuterated solvent as an internal reference. The following abbreviations were used to explain the multiplicities: s = singlet, d =doublet, t = triplet, q = quartet, m = multiplet, br = broad. Assignment of proton resonances was confirmed by correlated spectroscopy. Electrospray ionization high-resolution mass spectra (ESI-HRMS) were recorded on a Bruker MicroTOF II. IR spectra were obtained using an FT-IR Shimadzu spectrometer and only partial spectral data are listed. Melting points were measured on an Electrothermal 9100 apparatus and are uncorrected.

4.2. Synthesis

*4.2.1 Synthesis of N-propargyl methyl prolinate (**2**).*

To a solution of methyl prolinate (200 mg, 1.22 mmol) in 10 mL of $Et_2O_{(anh)}$, NEt_3 (439 mg, 4.3 mmol) and 80 % propargyl bromide in toluene (263 µL, 2.45 mmol) were added in this order and the reaction mixture was stirred at room temperature for 12 h. The solvent was evaporated, and the crude product was purified by column chromatography in silica gel with increasing ethyl acetate/hexane gradient to yield the expected product as a yellow oil (129 mg, 72 %).

^{1}H NMR (300 MHz, $CDCl_3$): δ 3.72 (s, 3H, OCH_3), 3.61 – 3.55 (m, 2H, C5-H, C2-H), 3.45–3.39 (m, 1H, C6-H), 3.07–3.01 (m, 1H, C6-H), 2.75–2.67 (m, 1H, C5-H), 2.20 -2.06 (m, 2H, C7-H and C3-H), 2.08–1.76 (m, 3H, C3-H, C4-H). ^{13}C NMR (75 MHz, $CDCl_3$): δ 173.9 (COO), 78.2 (C), 73.2 (CH), 62.4 (CH), 52.1 (CH_2), 51.9 (OCH_3), 41.1 (CH_2), 29.5 (CH_2), 23.2 (CH_2).

4.2.2. General procedure for the Cu(I) mediated 1,3-dipolar cycloaddition.

Propargyl methyl prolinate (1 eq) and the azide (1.1 eq) were suspended in 10 mL/eq of *t*BuOH:H_2O (1:1) and then 1M $CuSO_4$ solution and finally 1M sodium ascorbate solution were added and the mixture stirred overnight at room temperature. Brine was added, and the solution was extracted with dichloromethane. Combined organic extracts were dried over sodium sulfate and evaporated. Products were purified by column chromatography in silica gel with increasing Hexane/ethyl acetate/methanol gradients.

4.2.2.1 Methyl ((1-(2-ethoxy-2-oxoethyl)-1H-1,2,3-triazol-4-yl)methyl)-L-prolinate (**3a**). Compound **3a** was prepared from 45 mg (0.27 mmol) of N-propargyl methyl prolinate **1**, following the general procedure for the 1,3-dipolar cycloaddition, affording 66 mg of a yellowish oil in 80 % yield. ^{1}H NMR (300 MHz, $CDCl_3$): δ 7.62 (s, 1H, C7-H), 5.09 (d, *J* = 2.6 Hz, 2H, C8-H), 4.20 (q, *J* = 7.5 Hz, 2H, CH_2CH_3), 4.01 (d, *J* = 13.8 Hz, 1H, C6-H), 3.82 (d, *J* = 13.8 Hz, 1H, C6-H), 3.64 (s, 3H, OMe), 3.29 (dd, *J* = 8.7, *J* = 6.1 Hz, 1H, C2-H), 3.10 – 3.04 (m, 1H, C5-H), 2.50 (dt, *J* = 8.4 Hz, *J* = 8.2 Hz, 1H, C5-H), 2.07 – 1.74 (m, 4H, C3-H and C4-H), 1.23 (t, *J* = 7.5 Hz, 3H, CH_2CH_3). ^{13}C NMR (75 MHz, $CDCl_3$): δ 174.1 (C=O), 166.3 (C=O), 144.5 (C), 124.4 (CH), 64.4 (CH), 62.4 (CH_2), 53.0 (CH_2), 52.0 (CH_3), 50.8 (CH_2), 48.2 (CH_2), 29.3 (CH_2), 23.0 (CH_2), 14.0 (CH_3). IR (film): υ_{max} 3458, 3439, 2954,

2357, 1732, 1643, 1444, 1217, 1051, 1024, 875, 798, 756 cm^{-1}. ESI-HRMS *m/z* $[M+K]^+$ calcd for $C_{13}H_{20}KN_4O_4$ 335.1116, found 335.1113.

4.2.2.2 Methyl ((1-(5-ethoxy-5-oxopentyl)-1H-1,2,3-triazol-4-yl)methyl)-L-prolinate (**3b**). Compound **3b** was prepared from 45 mg (0.27 mmol) of N-propargyl methyl prolinate **1**, following the general procedure for the 1,3-dipolar cycloaddition, affording 63 mg of a yellowish oil in 69 % yield. ^{1}H NMR (300 MHz, $CDCl_3$): δ 7.50 (s, 1H, C7-H), 4.38 (d, *J* = 2.6 Hz, 2H, C8-H), 4.09 (q, *J* = 7.5 Hz, 2H, **CH$_2$**CH_3), 3.97 (d, *J* = 13.8 Hz, 1H, C6-H), 3.79 (d, *J* = 13.8 Hz, 1H, C6-H), 3.65 (3H, OMe), 3.28 (dd, *J* = 8.7, 6.1 Hz, 1H, C2-H), 3.12 – 3.07 (m, 1H, C5-H), 2.53 – 2.45 (m, 1H, C5-H), 2.32 – 2.08 (m, 6H, CH_2), 1.91 – 1.76 (m, 4H, C3-H and C4-H), 1.20 (t, *J* = 7.5 Hz, 3H, CH_2**CH$_3$**). ^{13}C NMR (75 MHz, $CDCl_3$): δ 174.4 (C=O), 172.3 (C=O), 144.5 (C6´), 122.8 (C7), 64.6 (C2), 60.6 (**CH$_2$**CH_3), 53.3 (C5), 51.8 (OCH_3), 49.1 (C8), 48.5 (C6), 30.6 (CH_2), 29.6 (CH_2), 29.3 (C3), 25.4 (C4), 23.0 (CH_2), 14.1 (CH_2**CH$_3$**). IR (film): υ_{max} 3437, 3138, 2954, 2358, 1730, 1633, 1444, 1377,1348, 1274, 1199, 1047, 1028, 854, 802 cm^{-1}. ESI-HRMS *m/z* $[M+H]^+$ calcd for $C_{16}H_{27}N_4O_4$ 339.2027, found 339.2029.

4.2.2.3 Methyl ((1-benzyl-1H-1,2,3-triazol-4-yl)methyl)-L-prolinate (**3c**). Compound **3c** was prepared from 45 mg (0.27 mmol) of N-propargyl methyl prolinate **1**, following the general procedure for the 1,3-dipolar cycloaddition, affording 66 mg of a yellowish oil in 80 % yield. ^{1}H NMR (300 MHz, $CDCl_3$): δ 7.42 (s,1H, C7-H), 7.36–7.30 (m, 3H, Ph), 7.27–7.21 (m, 2H, Ph), 5.48 (d, *J* = 2.6 Hz, 2H, C8-H), 3.95 (d, *J* = 13.8 Hz, 1H, C6-H), 3.78 (d, *J* = 13.8 Hz, 1H, C6-H), 3.60 (s, 3H, OMe), 3.27 (dd, *J* = 8.7, 6.1 Hz, 1H, C2-H), 3.09 (m, 1H, C5-H), 2.48 (dt, *J* = 8.4, 8.2 Hz, 1H, C5-H), 2.18–1.66 (m, 4H, C3-H and C4-H). ^{13}C NMR (75 MHz, $CDCl_3$): δ 174.6 (C=O), 145.1 (C6´), 134.8 (Ph, C), 129.2 (Ph, CH), 128.8 (Ph, CH), 128.3

(Ph, CH), 122.8 (C7), 64.9 (C2), 54.2 (C5), 53.5 (C8), 51.9 (OCH_3), 48.9 (C6), 29.5 (C3), 23.2 (C4). IR (film): υ_{max} 3493, 3140, 2951, 2850, 2359, 1745, 1732, 1556, 1496, 1454, 1359, 1284, 1049, 769, 725 cm^{-1}. ESI-HRMS *m/z* $[M+Na]^+$ calcd for $C_{16}H_{20}N_4NaO_2$ 323.1478, found 323.1474.

4.2.2.4 Methyl ((1-cyclohexyl-1H-1,2,3-triazol-4-yl)methyl)-L-prolinate (**3d**). Compound **3d** was prepared from 45 mg (0.27 mmol) of N-propargyl methyl prolinate **1**, following the general procedure for the 1,3-dipolar cycloaddition, affording 31 mg of a yellowish oil in 39% yield. ^1H NMR (300 MHz, $CDCl_3$): δ 7.51 (s, 1H, C7-H), 4.44 (d, *J* = 2.6 Hz, 2H, C8-H), 3.97 (d, *J* = 13.8 Hz, 1H, C6-H), 3.79 (d, *J* = 13.8 Hz, 1H, C6-H), 3.66 (s, 3H, OMe), 3.29 (dd, *J* = 8.7, 6.1 Hz, 1H, C2-H), 3.16 – 3.10 (m, 1H, C5-H), 2.46 (dt, *J* = 8.4, 8.2 Hz, 1H, C5-H), 2.20 – 1.63 (m, 12H, C3-H and cyclohexyl), 1.51 – 1.21 (m, 3H, C4-H and cyclohexyl). ^{13}C NMR (75 MHz, $CDCl_3$): δ 174.5 (C=O), 144.0 (C6′), 120.3 (C7), 64.8 (C2), 59.7 (C5), 53.4 (C8), 51.85 (OCH_3), 48.9 (C6), 33.5 (CH_2), 32.4 (C3), 29.4 (CH_2), 25.2 (CH_2), 23.0 (C4). IR (film): υ_{max} 3417, 3142, 2935, 2856, 2362, 1737, 1732, 1633, 1450, 1371, 1276, 1201, 1049, 997, 894, 823, 777 cm^{-1}. ESI-HRMS *m/z* $[M+H]^+$ calcd for $C_{15}H_{25}N_4O_2$ 293.1972, found 293.1970.

*4.2.2.5 Methyl ((1-(3-phenylpropyl)-1H-1,2,3-triazol-4-yl)methyl)-L-*prolinate (**3e**). Compound **3e** was prepared from 45 mg (0.27 mmol) of N-propargyl methyl prolinate **1**, following the general procedure for the 1,3-dipolar cycloaddition, affording 73 mg of a yellowish oil in 82% yield. ^1H NMR (300 MHz, $CDCl_3$): δ 7.43 (s, 1H, C7-H), 7.24 – 7.19 (m, 2H, Ph), 7.18 – 7.08 (m, 3H, Ph), 4.21 (d, *J* = 2.6 Hz, 2H, C8-H), 3.93 (d, *J* = 13.8 Hz, 1H, C6-H), 3.76 (d, *J* = 13.8 Hz, 1H, C6-H), 3.60 (s, 3H, OMe), 3.24 (dd, *J* = 8.7, 6.1 Hz,

1H, C2-H), 3.06 (m, 1H, C5-H), 2.53 – 2.44 (m, 5H), 2.23 – 1.61 (m, 4H, C3-H and C4-H). ^{13}C NMR (75 MHz, $CDCl_3$): δ 174.5 (C=O), 144.6 (C6´), 140.3 (Ph), 128.7 (Ph), 128.5 (Ph), 126.4 (Ph), 122.8 (C7), 64.7 (C2), 53.4 (C5), 51.9 (OCH_3), 49.5 (C8), 48.7 (C6), 32.5 (CH_2), 31.7 (C3), 29.5 (CH_2), 23.5 (C4). IR (film): υ_{max} 3626, 3458, 3138, 2949, 2854, 2358, 1732, 1602, 1496, 1444, 1354, 1278, 1172, 1085, 1049, 1004, 785, 748, 702 cm^{-1}. ESI-HRMS *m/z* $[M+Na]^+$ calcd for $C_{18}H_{24}N_4NaO_2$ 351.1791, found 351.1790.

4.2.2.6 Methyl ((1-cinnamyl-1H-1,2,3-triazol-4-yl)methyl)-L-prolinate (**3f**). Compound **3f** was prepared from 45 mg (0.27 mmol) of N-propargyl methyl prolinate **1**, following the general procedure for the 1,3-dipolar cycloaddition, affording 53 mg of a yellowish oil in 60% yield. ^{1}H NMR (300 MHz, $CDCl_3$): δ 7.58 (s, 1H, C7-H), 7.43 – 7.21 (m, 5H, Ph), 6.65 (d, *J* = 15.8 Hz, 1H, C9-H), 6.33 (m, 1H, C10-H), 5.11 (d, *J* = 2.6 Hz, 2H, C8-H), 4.00 (d, *J* = 13.8 Hz, 1H, C6-H), 3.82 (d, *J* = 13.8 Hz, 1H, C6-H), 3.66 (s, 3H, OMe), 3.31 (dd, *J* = 8.7, 6.1 Hz, 1H, C2-H), 3.14 (m, 1H, C5-H), 2.52 (dt, *J* = 8.4, 8.2 Hz, 1H, C5-H), 2.20 – 2.04 (m, 1H, C3-H), 2.00 – 1.71 (m, 3H, C3-H, C4-H_2). ^{13}C NMR (75 MHz, CDCl3): δ 174.5 (C=O), 144.9 (C6´), 135.3 (Ph), 135.3 (C9-H), 128.7 (Ph), 128.5 (CH), 126.7 (Ph), 122.5 (C10-H), 121.9 (C7), 64.7 (C2), 53.4 (C5), 52.3 (OCH_3), 51.8 (C8), 48.7 (C6), 29.4 (C3), 23.0 (C4). IR (film): υ_{max} 3541, 3138, 2951, 2845, 2358, 1741, 1732, 1552, 1448, 1359, 1278, 1203, 1174, 1128, 1047, 970, 756, 694 cm^{-1}. ESI-HRMS *m/z* $[M+Na]^+$ calcd for $C_{18}H_{22}N_4NaO_2$ 349.1635, found 349.1625.

4.2.2.7 Methyl ((1-(naphthalen-2-ylmethyl)-1H-1,2,3-triazol-4-yl)methyl)-L-prolinate (**3g**). Compound **3g** was prepared from 20 mg (0.12 mmol) of N-propargyl methyl prolinate **1**, following the general procedure for the 1,3-dipolar cycloaddition, affording 34 mg of a light orange solid in 81% yield. M.p. 64.0-64.9 ºC. ^{1}H NMR (300 MHz, $CDCl_3$): δ 7.85 – 7.82 (m,

3H, naphtyl), 7.74 (s, 1H, C-H), 7.52 – 7.49 (m, 2H, naphtyl), 7.46 (s, 1H, C7-H), 7.37 – 7.33 (m, 1H, naphtyl), 5.66 (d, *J* = 3.6 Hz, 2H, C8-H), 3.97 (d, *J* = 13.9 Hz, 1H, C6-H), 3.80 (d, *J* = 13.9 Hz, 1H, C6-H), 3.60 (s, 3H, OMe), 3.26 (dd, *J* = 8.7, 6.1 Hz, 1H, C2-H), 3.06 (m, 1H, C5-H), 2.46 (dt, *J* = 8.4, 8.2 Hz, 1H, C5-H), 2.15 – 1.65 (m, 4H, C3-H and C4-H). ^{13}C NMR (75 MHz, CDCl3): δ 174.4 (C=O), 145.1 (C6´), 133.2 (C), 133.1 (C), 131.9 (C), 129.1 (CH), 127.9 (CH), 127.7 (CH), 127.4 (CH), 126.7 (CH), 125.3 (C7), 122.7 (CH), 122.7 (CH), 64.7 (C2), 54.3 (C5), 53.4 (C8), 51.8 (OCH_3), 43.7 (C6), 29.4 (C3), 23.0 (C4). IR (KBr): υ_{max} 3500, 3132, 2949, 2818, 2358, 1732, 1600, 1548, 1508, 1435, 1338, 1273, 1203, 1172, 1126, 1047, 891, 771 cm^{-1}. ESI-HRMS *m/z* $[M+H]^+$ calcd for $C_{20}H_{23}N_4O_2$ 351.1815, found 351.1826.

4.2.2.8 Methyl ((1-octyl-1H-1,2,3-triazol-4-yl)methyl)-L-prolinate (**3h**). Compound **3h** was prepared from 20 mg (0.12 mmol) of N-propargyl methyl prolinate **1**, following the general procedure for the 1,3-dipolar cycloaddition, affording 31 mg of a yellow oil in 81% yield. ^{1}H NMR (300 MHz, $CDCl_3$): δ 7.44 (s, 1H, C7-H), 4.24 (t, *J* = 7.2 Hz, 2H, C8-H), 3.93 (d, *J* = 13.8 Hz, 1H, C6-H), 3.75 (d, *J* = 13.8 Hz, 1H, C6-H), 3.61 (s,3H, OMe), 3.23 (dd, *J* = 8.6, 6.0 Hz, 1H, C2-H), 3.08 – 3.02 (m, 1H, C5-H), 2.49 – 2.41 (dt, 1H, *J* = 8.4, 8.1 Hz, C5-H), 2.03 – 1.71 (m, 5H), 1.22 – 1.17 (m, 11H), 0.79 (t, *J*= 6.5 Hz, 3H, CH_3). ^{13}C NMR (75 MHz, $CDCl_3$): δ 174.4 (C=O), 144.4 (C6´), 122.5 (C7), 64.6 (C2), 53.2 (C5), 51.8 (OCH_3), 50.2 (C8), 48.6 (C6), 31.6 (CH_2), 30.2 CH_2), 29.4 (C3), 29.0 (CH_2), 28.9 (CH_2), 26.4 (CH_2), 23.0 (C4), 22.5 (CH_2), 14.0 (CH_3). IR (film): υ_{max} 3604, 3458, 3136, 2926, 2357, 1345, 1645, 1444, 1354, 1172, 1047, 771 cm^{-1}. ESI-HRMS *m/z* $[M+Na]^+$ calcd for $C_{17}H_{30}N_4NaO_2$ 345.2261, found 345.2261.

4.2.2.9 Methyl ((1-decyl-1H-1,2,3-triazol-4-yl)methyl)-L-prolinate (**3i**). Compound **3i** was prepared from 20 mg (0.12 mmol) of N-propargyl methyl prolinate **1**, following the general procedure for the 1,3-dipolar cycloaddition, affording 32 mg of a yellow oil in 75% yield. ^{1}H NMR (300 MHz, $CDCl_3$): δ 7.49 (s, 1H, C7-H), 4.32 (t, *J* = 7.2 Hz, 2H, C8-H), 4.02 (d, *J* = 13.8 Hz, 1H, C6-H), 3.83 (d, *J* = 13.8 Hz, 1H, C6-H), 3.66 (s, 3H, OMe), 3.33 (dd, *J* = 8.7, 6.1 Hz, 1H, C2-H), 3.17 – 3.08 (m, 1H, C5-H), 2.58 – 2.50 (dt, *J* = 8.4, 8.2 Hz, 1H, C5-H), 2.11 – 1.77 (m, 4H, C3-H and C4-H), 1.27 – 1.21 (m, 16H), 0.84 (t, *J* = 6.6 Hz, 3H, CH_3). ^{13}C NMR (75 MHz, $CDCl_3$): δ 174.5 (C=O), 144.4 (C6´), 122.7 (C7), 64.7 (C2), 53.4 (C5), 51.9 (OCH_3), 50.4 (C8), 48.7 (C6), 31.9 (CH_2), 30.4 (CH_2), 29.5 (C3), 29.5 (CH_2), 29.3 (CH_2), 29.1 (CH_2), 29.1 (CH_2), 26.5 (CH_2), 23.1 (C4), 22.7 (CH_2), 14.2 (CH_3). IR (film): υ_{max} 3458, 2926, 2854, 2358, 1745, 1732, 1651, 1444, 1373, 1278, 1199, 1172, 1047, 891, 783, 721 cm^{-1}. ESI-HRMS *m/z* $[M+H]^+$ calcd for $C_{19}H_{35}N_4O_2$ 351.2754, found 351.2746.

4.2.2.10 Methyl ((1-hexadecyl-1H-1,2,3-triazol-4-yl)methyl)-L-prolinate (**3j**). Compound **3j** was prepared from 20 mg (0.12 mmol) of N-propargyl methyl prolinate **1**, following the general procedure for the 1,3-dipolar cycloaddition, affording 22 mg of a white solid in 42 % yield. M.p. 60-60.9 ºC. ^{1}H NMR (300 MHz, $CDCl_3$): δ 7.47 (s, 1H, C7-H), 4.29 (t, *J* = 7.2 Hz, 2H, C8-H), 3.99 (d, *J* = 13.8 Hz, 1H, C6-H), 3.80 (d, *J* = 13.8 Hz, 1H, C6-H), 3.67 (s, 3H, OMe), 3.30 (dd, *J* = 8.7, 6.1 Hz, 1H, C2-H), 3.16 – 3.11 (m, 1H, C5-H), 2.57 – 2.48 (dt, *J* = 8.9, 7.8 Hz, 1H, C5- H), 1.91 – 1.84 (m, 4H), 1.28 – 1.23 (m, 28H), 0.85 (t, *J* = 6.6 Hz, 3H, CH_3). ^{13}C NMR (75 MHz, $CDCl_3$): δ 174.7 (C=O), 144.7 (C6´), 122.6 (C7), 64.6 (C2), 53.2 (C5), 52.0 (OCH_3), 50.5 (C8), 48.9 (C6), 32.1 (CH_2), 30.5 (CH_2), 29.9 (CH_2), 29.8 (CH_2), 29.8 (CH_2), 29.7 (CH_2), 29.6 (CH_2), 29.6 (CH_2), 29.6 (CH_2), 29.4 (C3), 29.3 (CH_2), 29.2 (CH_2), 28.9 (CH_2), 26.4 (CH_2), 23.0 (C4), 22.6 (CH_2), 14.0 (CH_3). IR (KBr): υ_{max} 3124,

2914, 2357, 1745, 1728, 1556, 1444, 1336, 1269, 1197, 1053, 848, 790, 719 cm^{-1}. ESI-HRMS *m/z* $[M+Na]^+$ calcd for $C_{25}H_{46}N_4NaO_2$ 457.3513, found 457.3512.

4.2.2.11 Methyl (Z)-((1-(octadec-9-en-1-yl)-1H-1,2,3-triazol-4-yl)methyl)-L-prolinate **(3k).** Compound **3k** was prepared from 20 mg (0.12 mmol) of N-propargyl methyl prolinate **1**, following the general procedure for the 1,3-dipolar cycloaddition, affording 33 mg of a light-yellow oil in 59 % yield. ^1H NMR (300 MHz, $CDCl_3$): δ 7.49 (s, 1H, C7-H), 5.35 – 5.31 (m, CH=CH, 2H), 4.30 (t, *J* = 7.2 Hz, 2H, C8-H), 4.00 (d, *J* = 13.8 Hz, 1H, C6-H), 3.81 (d, *J* = 13.8 Hz, 1H, C6-H), 3.68 (s, 3H, OMe), 3.30 (dd, *J* = 8.8, 6.1 Hz, 1H, C2-H), 3.15 – 3.10 (m, 1H, C5-H), 2.56 – 2.48 (dt, *J* = 8.5, 8.1 Hz, 1H, C5-H), 2.16 – 1.79 (m, 6H), 1.27 – 1.25 (m, 26H), 0.87 (t, *J* = 6.7 Hz, 3H, CH_3). ^{13}C NMR (75 MHz, $CDCl_3$): δ 174.4 (C=O), 144.4 (C6´), 130.0 (CH=), 129.7 (CH=), 122.5 (C7), 64.7 (C2), 53.3 (C5), 51.8 (OCH_3), 50.3 (C8), 48.6 (C6), 31.9 (CH_2), 30.3 (CH_2), 29.7 (CH_2), 29.7 (CH_2), 29.5 (C3), 29.4 (CH_2), 29.4 (CH_2), 29.3 (CH_2), 29.1 (CH_2), 29.0 (CH_2), 29.0 (CH_2), 27.2 (CH_2), 27.1 (CH_2), 26.5 (CH_2), 23.0 (C4), 22.6 (CH_2), 14.1 (CH_3).IR (film): υ_{max} 3564, 3477, 3136, 2924, 2852, 2358, 2096, 1745, 1556, 1444, 1373, 1276, 1199, 1172, 1047, 968, 891, 775, 723 cm^{-1}. ESI-HRMS *m/z* $[M+K]^+$ calcd for $C_{27}H_{48}KN_4O_2$ 499.3408, found 499.3412.

4.2.2.12 Methyl ((1-icosyl-1H-1,2,3-triazol-4-yl)methyl)-L-prolinate (**3l**). Compound **3l** was prepared from 20 mg (0.12 mmol) of N-propargyl methyl prolinate **1**, following the general procedure for the 1,3-dipolar cycloaddition, affording 34 mg of a white solid in 58 % yield. M.p. 72.7-73.7 ºC. ^1H NMR (300 MHz, $CDCl_3$): δ 7.49 (s, 1H, C7-H), 4.31 (t, *J* = 7.2 Hz, 2H, C8-H), 4.01 (d, *J* = 13.8 Hz, 1H, C6-H), 3.82 (d, *J* = 13.8 Hz, 1H, C6-H), 3.69 (s, 3H, OMe), 3.30 (dd, *J* = 8.5, 5.7 Hz, 1H, C2-H), 3.14 – 3.1 (m, 1H, C5-H), 2.54 – 2.46 (dt, *J* = 8.5, 7.9 Hz, 1H, C5- H), 1.91 – 1.84 (m, 4H), 1.28 – 1.23 (m, 36H), 0.87 (t, *J* = 6.7 Hz, 3H,

CH_3). ^{13}C NMR (75 MHz, $CDCl_3$): δ 174.5 (C=O), 144.4 (C6'), 122.4 (C7), 64.7 (C2), 53.3 (C5), 51.8 (OMe), 50.2 (C8), 48.6 (CH_2), 31.9 (CH_2), 30.2 (CH_2), 29.6 (CH_2), 29.5 (CH_2), 29.3 (CH_2), 29.0 (CH_2), 26.4 (CH_2), 23.0 (CH_2), 22.6 (CH_2), 14.1 (CH_3). IR (KBr): υ_{max} 3649, 3124, 3076, 2916, 2846, 2358, 1743, 1462, 1338, 1271, 1211, 1055, 1037, 852, 771, 719 cm^{-1}. ESI-HRMS *m/z* $[M+Na]^+$ calcd for $C_{29}H_{54}NaN_4O_2$ 513.4139, found 513.4125.

4.2.2.13 Methyl ((1-(3,7-dimethylocta-2,6-dien-1-yl)-1H-1,2,3-triazol-4-yl)methyl)-L-prolinate (**3m**). Compound **3m** was prepared from 30 mg (0.18 mmol) of N-propargyl methyl prolinate **1**, following the general procedure for the 1,3-dipolar cycloaddition, affording 47 mg of a yellow oil in 87 % yield. ^1H NMR (300 MHz, $CDCl_3$): δ 7.46 (s, 1H, C7-H), 5.41 (t, *J* = 7.2 Hz, 1H, C9-H), 5.08 – 5.01 (m, 1H, C13-H), 4.90 (t, *J* = 7.2 Hz, 2H, C8-H), 4.01 (d, *J* = 13.6 Hz, 1H, C6-H), 3.82 (d, *J* = 13.6 Hz, 1H, C6-H), 3.66 (s, 3H, OMe), 3.30 (dd, *J* = 8.1, 6.0 Hz, 1H, C2-H), 3.12 – 3.1 (m, 1H, C5-H), 2.54 – 2.46 (dt, *J* = 8.4, 8.2 Hz, 2H, C5-H), 1.7 (m, 6H, C3-H and C4-H), 1.65 (s, 3H, CH_3), 1.63 (m, 6H, CH_3), 1.55 (m, 3H, CH_3). ^{13}C NMR (75 MHz, $CDCl_3$): δ 174.5 (C=O), 144.4 (C6´), 122.7 (C7), 64.7 (C2), 53.4 (C5), 51.9 (OCH_3), 50.4 (C8), 48.7 (C6), 31.9 CH_2), 30.4 (CH_2), 29.5 (C3), 29.3 (CH_2), 29.1 (CH_2), 26.5 (CH_2), 23.1 (C4), 22.7 (CH_2), 17.6 (CH_3), 16.5 (CH_3), 16.0 (CH_3). IR (film): υ_{max} 3564, 3140, 2926, 2358, 1867, 1747, 1732, 1506, 1435, 1373, 1217, 1174, 1124, 1047, 844, 771 cm^{-1}. ESI-HRMS *m/z* $[M+H]^+$ calcd for $C_{19}H_{35}N_4O_2$ 351.2754, found 351.2746.

4.2.2.14 Methyl ((1-((2E,6E)-3,7,11-trimethyldodeca-2,6,10-trien-1-yl)-1H-1,2,3-triazol-4-yl)methyl)-L-prolinate (**3n**) and *Methyl ((1-((2E,6Z)-3,7,11-trimethyldodeca-2,6,10-trien-1-yl)-1H-1,2,3-triazol-4-yl)methyl)-L-prolinate* (**3o**). Compound **3n** and **3o** were prepared from 50 mg (0.30 mmol) of N-propargyl methyl prolinate **1**, following the general procedure for

the 1,3-dipolar cycloaddition, affording 53 mg of **3n** and 28 mg of **3o** as yellowish oils in 43 % and 23% yield, respectively.

3n - ^{1}H NMR (300 MHz, $CDCl_3$): δ 7.47 (s, 1H, C7-H), 5.42 (t, *J* = 7.2 Hz, 1H, C9-H), 5.08 – 5.06 (m, 2H, C13-H and C16-H), 4.95 (t, *J* = 7.2 Hz, 2H, C8-H), 4.00 (d, *J* = 13.7 Hz, 1H, C6-H), 3.80 (d, *J* = 13.7 Hz, 1H, C6-H), 3.69 (s, 3H, OMe), 3.31 (dd, *J* = 8.7, 6.1 Hz, 1H, C2-H), 3.16 – 3.10 (m, 1H,C5-H), 2.61 – 2.48 (dt, *J* = 8.4, 8.2 Hz, 1H, C5-H), 1.70 (m, 4H, C3-H and C4-H), 2.12 – 1.91 (m, 8H), 1.78 (s, 3H, CH_3), 1.65 (s, 3H, CH_3), 1.63 (m, 3H, CH_3), 1.55 (m, 3H, CH_3). ^{13}C NMR (75 MHz, $CDCl_3$): δ 174.4 (C=O), 144.4 (C6´), 143.1 (C), 135.7 (C), 131.3 (C), 124.2 (CH), 123.3 (CH), 122.0 (C7-H), 116.9 (CH), 64.7 (C2), 53.2 (C5), 51.8 (OCH_3), 48.6 (C8), 47.8 (C6), 39.6 (CH_2), 39.4 (CH_2), 29.3 (C3), 26.6 (CH_2), 26.1 (CH_2), 25.6 (CH_2), 22.9 (CH_3), 17.6 (CH_3), 16.5 (CH_3), 16.0 (CH_3). IR (film): υ_{max} 3417, 3124, 2992, 2358, 1867, 1747, 1732, 1539, 1456, 1317, 1271, 1122, 1047, 773 cm^{-1}. ESI-HRMS *m/z* $[M+H]^+$ calcd for $C_{24}H_{39}N_4O_2$ 415.3067, found 415.3067.

3o - ^{1}H NMR (300 MHz, $CDCl_3$): δ 7.47 (s, 1H, C7-H), 5.42 (t, *J* = 7.2 Hz, 1H, C9-H), 5.08 – 5.06 (m, 2H, C13-H and C16-H), 4.95 (t, *J* = 7.2 Hz, 2H, C8-H), 4.00 (d, *J* = 13.7 Hz, 1H, C6-H), 3.80 (d, *J* = 13.7 Hz, 1H, C6-H), 3.69 (s,3H, OMe), 3.31 (dd, *J* = 8.7, 6.1 Hz, 1H, C2-H), 3.16 – 3.10 (m, 1H, C5-H), 2.61 – 2.48 (dt, *J* = 8.4, 8.2 Hz, 1H, C5-H), 1.7 (m, 4H, C3-H and C4-H), 2.12 – 1.91 (m, 8H), 1.78 (s, 3H, CH_3), 1.65 (s, 3H, CH_3), 1.63 (m, 3H, CH_3), 1.55 (m, 3H, CH_3). ^{13}C NMR (75 MHz, $CDCl_3$): δ 174.4 (C=O), 144.4 (C6´), 143.1 (C), 135.7 (C), 131.3 (C), 124.2 (CH), 123.3 (CH), 122.0 (C7-H), 116.9 (CH), 64.7 (C2), 53.2 (C5), 51.8 (OCH_3), 48.6 (C8), 47.8 (C6), 39.6 (CH_2), 39.4 (CH_2), 29.3 (C3), 26.6 (CH_2), 26.1 (CH_2), 25.6 (CH_2), 22.9 (CH_3), 17.6 (CH_3), 16.5 (CH_3), 16.0 (CH_3). IR (film): υ_{max} 3417,

3124, 2962, 2924, 2341, 1745, 1732, 1625, 1446, 1435, 1377, 1215, 1172, 1047, 775 cm^{-1}. ESI-HRMS *m/z* $[M+H]^+$ calcd for $C_{24}H_{39}N_4O_2$ 415.3067, found 415.3067.

4.2.2.15 Methyl ((1-((E)-3,7,11,15-tetramethylhexadec-2-en-1-yl)-1H-1,2,3-triazol-4-yl)methyl) -L-prolinate (**3p**) and *Methyl ((1-(3,7,11,15-tetramethylhexadec-2-en-1-yl)-1H-1,2,3-triazol-4-yl)methyl)-L-prolinate* (**3q**). Compound **3p** and **3q** were prepared from 50 mg (0.30 mmol) of N-propargyl methyl prolinate **1**, following the general procedure for the 1,3-dipolar cycloaddition, affording 22 mg of **3p** (*E*-isomer) and 23 mg of **3q** (mixture *E: Z*) as yellowish oils in 38 % and 39 % yield, respectively.

3p - ^{1}H NMR (300 MHz, $CDCl_3$): δ 7.47 (s, 1H, C7-H), 5.39 (t, *J* = 7.2 Hz, 1H, C9-H), 4.91 (t, *J* = 7.2 Hz, 2H, C8-H), 3.98 (d, *J* = 13.7 Hz, 1H, C6-H), 3.78 (d, *J* = 13.7 Hz, 1H, C6-H), 3.68 (s, 3H, OMe), 3.29 (dd, *J* = 8.7, 6.1 Hz, 1H, C2-H), 3.14 – 3.09 (m, 1H, C5-H), 2.54 – 2.46 (dt, *J* = 8.4, 8.2 Hz, 1H, C5-H), 2.11 (s, 3H, C10-CH_3), 2.02 – 1.84 (m, 4H, C3-H and C4-H), 1.77 – 1.75 (m, 3H), 1.36 – 1.06 (m, 18H), 0.86 – 0.81 (m, 12H, CH_3). ^{13}C NMR (75 MHz, $CDCl_3$): δ 174.4 (C=O), 144.4 (C6´), 143.7 (C10), 122.1 (C7), 117.4 (C9), 64.8 (C2), 53.7 (C5), 51.9 (OCH_3), 48.7 (C6), 39.8 (C8), 39.4 (CH_2), 37.4 (CH_2), 37.3 (CH_2), 37.0 (CH_2), 36.9 (CH_2), 36.7 (CH_2), 32.7 (CH_2), 32.3 (CH_2), 29.7 (C3), 29.4 (C4), 28.0 (CH_2), 25.5 (CH_2), 25.0 (CH_2), 24.8 (CH_2), 24.5 (CH_3), 23.4 (CH_3), 23.0 (CH_3), 22.7 (CH_3), 22.6 (CH_3). IR (film): υ_{max} 3500, 3140, 2926, 2358, 1747, 1506, 1456, 1377, 1172, 1047, 933, 862, 775 cm^{-1}. ESI-HRMS: mass calculated for $C_{29}H_{52}N_4NaO_2$ $(M+Na)^+$, 511.3982, found 511.3970.

3q - ^{1}H NMR (300 MHz, $CDCl_3$): δ 7.47 (s, 1H, C7-H), 5.39 (t, *J* = 7.2 Hz, 1H, CH), 4.91 (t, *J* = 7.2 Hz, 2H, C8-H), 3.98 (d, *J* = 13.7 Hz, 1H, C6-H), 3.78 (d, *J* = 13.7 Hz, 1H, C6-H),

3.68 (s,3H, OMe), 3.29 (dd, *J* = 8.7, 6.1 Hz, 1H, C2-H), 3.14 – 3.09 (m, 1H, C5-H), 2.54 – 2.46 (dt, *J* = 8.4 Hz, *J* = 8.2 Hz, 1H, C5-H), 2.11 (s, 3H, CH_3), 2.02 – 1.84 (m, 4H, C3-H and C4-H), 1.77 – 1.75 (m, 3H), 1.36 – 1.06 (m, 18H), 0.86 – 0.81 (m, 12H, CH_3). ^{13}C NMR (75 MHz, $CDCl_3$): δ 174.4 (C=O), 144.4 (C6´), 143.7 (C10), 122.1 (C7), 117.4 (C9), 64.8 (C2), 53.7 (C5), 51.9 (OCH_3), 48.7 (C6), 39.8 (C8), 39.4 (CH_2), 37.4 (CH_2), 37.3 (CH_2), 37.0 (CH_2), 36.9 (CH_2), 36.7 (CH_2), 32.7 (CH_2), 32.3 (CH_2), 29.7 (C3), 29.4 (C4), 28.0 (CH_2), 25.5 (CH_2), 25.0 (CH_2), 24.8 (CH_2), 24.5 (CH_3), 23.4 (CH_3), 23.0 (CH_3), 22.7 (CH_3), 22.6 (CH_3). IR (film): υ_{max} 3500, 3140, 2926, 2358, 1747, 1506, 1456, 1377, 1172, 1047, 933, 862, 775 cm^{-1}. ESI-HRMS *m/z* $[M+Na]^+$ calcd for $C_{29}H_{52}N_4NaO_2$ 511.3982, found 511.3970.

4.2.2.16 Synthesis of N-(10-azidodecyl)-7-nitrobenzo[c][1,2,5]oxadiazol-4-amine. (**7**)

NBD-Cl (138 mg, 0,69 mmol) was dissolved in 2 mL of THF, then 10-azido-1-decylamine (150 mg, 0.75 mmol), Cs_2CO_3 (97 mg, 0,69 mmol) were added and the solution stirred at 50 °C for 4 h. Distillated water was added (20 mL), and the solution was extracted with ethyl acetate (3 x 10 mL). Combined organic extracts were dried over sodium sulfate and evaporated. The product was purified by column chromatography in silica gel with increasing ethyl acetate/hexane mixture.

^{1}H NMR (300 MHz, $CDCl_3$): δ 8.51 (d, *J* = 9.1 Hz, 1H, NBD), 6.18 (d, *J* = 9.1 Hz, 1H, NBD), 3.49 (dd, *J* = 13.2, 6.3 Hz, 2H, C1-H), 3.25 (t, *J* = 6.9, 2H, C10-H), 1.86 – 1.76 (m, 2H), 1.64 – 1.25 (m, 14H). ^{13}C NMR (75 MHz. $CDCl_3$): δ = 144.3 (C), 143.9 (C), 143.8 (C), 136.4 (CH), 124.1 (C), 98.5 (CH), 51.4 (C1), 44.0 (C10), 29.3 (CH_2), 29.2 (CH_2), 29.1 (CH_2), 28.8 (CH_2), 28.6 (CH_2), 28.5 (CH_2), 26.9 (CH_2), 26.7 (CH_2).

4.2.2.17 Methyl ((1-(10-((7-nitrobenzo[c][1,2,5]oxadiazol-4-yl)amino)decyl)-1H-1,2,3-triazol-4-yl)methyl)-L-prolinate (**3i-NBD**).

Compound **3i-NBD** was prepared following the general procedure for the 1,3-dipolar cycloaddition by reaction of azido-NBD **7** (20 mg, 0.055 mmol) and N-propargyl methyl prolinate (20 mg, 0.12 mmol) affording 17 mg of a yellow oil in 58 % yield. ^{1}H NMR (300 MHz, $CDCl_3$): δ 8.50 (d, *J* = 9.1 Hz, 1H, NBD), 7.51 (s, 1H, C7-H), 6.18 (d, *J* = 9.1 Hz, 1H, NBD), 4.33 (t, *J* = 7.2 Hz, 2H, C8-H), 4.01 (d, *J* = 13.8 Hz, C6-H, 1H), 3.82 (d, *J* = 13.8 Hz, 1H, C6-H,), 3.69 (s, 3H, OMe), 3.50 (dd, *J* = 8.5, 5.7 Hz, C17-H, 2H), 3.34 – 3.29 (m, 1H, C2), 3.16 – 3.11 (m, 1H, C5), 2.54 – 2.51 (m, 1H, C5), 2.00 – 1.67 (m, 6H), 1.30 (s, 14H). ^{13}C NMR (75 MHz, $CDCl_3$): δ 174.5 (C=O), 144.7 (C), 144.3 (C), 143.9 (C), 136.8 (=C-H), 123.5 (C), 122.7 (C7), 98.5 (=C-H), 64.8 (C2), 53.4 (C5), 51.9 (OMe), 50.2 (CH_2), 48.8 (C6), 44.0 (CH_2), 30.1 (C3), 29.4 (CH_2), 29.0 (CH_2), 28.9(CH_2), 28.7 (CH_2), 28.7 (CH_2), 28.4 (CH_2), 28.4 (CH_2), 26.8 (CH_2), 26.2 (CH_2), 23.1 (CH_2).

4.3. Biology

4.3.1 Reagents

All reagents were purchased from Sigma-Aldrich (St. Louis, MO, USA). Culture medium and fetal calf serum (FCS) were purchased from Cultilab (Campinas, SP, Brazil).

4.3.2. Cells and parasites

T. cruzi CL strain clone 14 epimastigotes[69] were maintained in the exponential growth phase by subculturing every 48 h in Liver Infusion Tryptose (LIT) medium[70] supplemented with 10% FCS (Vitrocell, Campinas, São Paulo, Brazil) at 28 °C.

4.3.3. Growth inhibition assays

T. cruzi epimastigotes in the exponential growth phase (5.0-6.0 x 10^7 cells mL^{-1}) were cultured in fresh LIT medium. The cells were treated with different concentrations of drugs

or not treated (negative control). A combination of Rotenone (60 µM) and Antimycin (0.5 µM) was used as a positive control for inhibition as previously described.[21] The cells (2.5 x 10^6 mL^{-1}) were transferred to 96-well culture plates and incubated at 28 °C. Cell proliferation was quantified by reading the optical density (OD) at 620 nm for eight days. The OD was converted to cell density values (cells per mL) using a linear regression equation previously obtained under the same conditions. The concentration of compounds that inhibited 50% of parasite proliferation (IC_{50}) was determined during the exponential growth phase (four days) by fitting the data to a typical sigmoidal dose-response curve using OriginPro8. The compounds were evaluated in quadruplicate in each experiment. The results shown here correspond to three independent experiments. As a cell growth inhibition control, growth curves in which 200 mM rotenone and 0.5 mM antimycin were added to the culture medium were run in parallel for all experiments.

4.3.4. Statistical analysis

One-way ANOVA followed by the Tukey test was used for statistical analysis. The *T* test was used to analyze differences between groups. $P<0.05$ was considered statistically significant.

4.3.5. Cytotoxicity assay

To evaluate the analogs toxicity, Vero cells previously plated on 96 multi-well plate in DMEM 2% FBS and incubated for 48 hours at 37 °C in a humid atmosphere containing 5% CO_2, were incubated with 700 µL of DMEM 2% FBS supplemented with each analog for 48 hours. The concentration (µM) was different with each analog:

- 3i: 20uM, 40uM, 60uM, 80uM, 100uM y 120uM.
- 3k: 5uM, 10uM, 15uM, 20uM, 25uM y 30uM.
- 3n: 5uM, 10uM, 15uM, 20uM, 25uM y 30uM.

- DMSO: 5uM, 25uM, 50uM y 100uM.
- Benznidazol: 10uM, 100uM, 200uM y 300uM.

The viability of cells was measured by MTT dye (3-(4,5-Dimethylthiazol-2-yl)-2,5-diphenyltratazolium Bromide, Sigma-Aldrich) colorimetric method. Benznidazole and DMSO were used as positive and negative controls, respectively. Data are expressed as means ± SD of the results of three independent assays of each condition.

4.3.6. Transport Assay

Two-day cultured parasites were washed three times by centrifugation and resuspended in phosphate buffered saline (PBS), pH 7.4. Cells were counted in a Neubauer chamber, adjusted with the same buffer to a final density of $200x10^6$ cells/mL and distributed in aliquots of 100 µL (containing 20 $x10^6$ cells each). Transport assays were initiated by the addition to the assay tubes of 100 µl of the desired dilution of L-proline in PBS in the presence of 0.5 mCi of L-[3H] proline. Unless otherwise specified, V0 was measured at 28 °C for 30 s by incorporation of 0.75 and 3 mM L-proline traced with 1 µCi of U-^{14}C-L-Pro (Perkin Elmer). In all cases, proline transport was stopped by addition of 800mL of cold 50 mM proline in PBS (pH 7.4), and rapid washing by centrifugation at 10,000x *g* for 2 minutes. Background values in each experiment were measured by simultaneous addition of radiolabeled L-proline and stop solution as previously described.[24]

4.3.7. Competition assay

For the competition assays, the transport experiments were performed as described above using the L-Pro concentration corresponding to the K_m (0.31 mM). Those conditions were chosen considering an inhibitory activity by structurally related compounds should be competitive, and so, should be evidenced by a change in the V_{max} at L-Pro concentrations

close to the K_m. Non-competitive inhibitors, if any, should diminish V_{max}, which is measured at 10 x K_m L-Pro (3.1 mM).

4.3.7. Confocal microscopy

The epimastigotes were fixed with 500 μL of formaldehyde 3.7% (w/v) in PBS. Then they were washed twice with PBS, suspended in 40 μL of PBS, settled on polylysine-coated coverslips and mounted with VectaShield reagent. All the images were acquired with a confocal Zeiss LSM880 microscope and using Zeiss Zen software. The emission of the samples displaying green fluorescence (treated with **3i-NBD**) was registered at 490/535 nm under Argon laser excitation (488 nm). The emission of the samples treated with DAPI was registered at 430/50 nm under ~~Argon~~ laser excitation (405 nm).. All the images were processed using the ImageJ software. [71, 72]

Acknowledgements

The authors wish to express their gratitude to UNR (Universidad Nacional de Rosario), CONICET (Consejo Nacional de Investigaciones Científicas y Técnicas, PIP 2009-11/0796 and PIP 2012-14/0448 awarded to G.R.L.), Agencia Nacional de Promoción Científica y Tecnológica (ANPCyT PICT- 2011-0589 awarded to G.R.L.) and Fundación Bunge y Born (FBB 31/10 awarded to G.R.L.), Fundação de Amparo à Pesquisa do Estado de São Paulo grants 2016/06034-2 (awarded to A.M.S.), Conselho Nacional de Pesquisas Científicas e Tecnológicas (CNPq) grants 404769/2018-7 and 308351/2013-4 (awarded to A.M.S.), and the Research Council United Kingdom Global Challenges Research Fund under grant agreement "A Global Network for Neglected Tropical Diseases" (grant MR/P027989/1). GRL and JAC are members of the Research Career of the Consejo Nacional de

Investigaciones Científicas y Técnicas of Argentina (CONICET). L.F., E.A.P.Z and L.P. thanks CONICET for the award of a Fellowship.

References

[1] M.C.P. Nunes, W. Dones, C.A. Morillo, J.J. Encina, A.L. Ribeiro, Chagas Disease: An Overview of Clinical and Epidemiological Aspects, J. Am. Coll. Cardiol., 62 (2013) 767-776.

[2] J.A. Pérez-Molina, I. Molina, Chagas disease, The Lancet, 391 (2018) 82-94.

[3] J.A. Urbina, Specific chemotherapy of Chagas disease: Relevance, current limitations and new approaches, Acta Trop., 115 (2010) 55-68.

[4] P.M.M. Guedes, G.K. Silva, F.R.S. Gutierrez, J.S. Silva, Current status of Chagas disease chemotherapy, Expert Rev. Anti Infect. Ther., 9 (2011) 609-620.

[5] L. Marchese, J. Nascimento, F. Damasceno, F. Bringaud, P. Michels, A. Silber, The Uptake and Metabolism of Amino Acids, and Their Unique Role in the Biology of Pathogenic Trypanosomatids, Pathogens, 7 (2018) 36.

[6] C.A. Pereira, G.D. Alonso, M.C. Paveto, A. Iribarren, M.L. Cabanas, H.N. Torres, M.M. Flawiá, Trypanosoma cruzi Arginine Kinase Characterization and Cloning: A NOVEL ENERGETIC PATHWAY IN PROTOZOAN PARASITES, J. Biol. Chem., 275 (2000) 1495-1501.

[7] M. Crispim, F.S. Damasceno, A. Hernández, M.J. Barisón, I. Pretto Sauter, R. Souza Pavani, A. Santos Moura, E.M.F. Pral, M. Cortez, M.C. Elias, A.M. Silber, The glutamine synthetase of Trypanosoma cruzi is required for its resistance to ammonium accumulation and evasion of the parasitophorous vacuole during host-cell infection, PLOS Neglected Tropical Diseases, 12 (2018) e0006170.

[8] R.M.B.M. Girard, M. Crispim, M.B. Alencar, A.M. Silber, Uptake of L-Alanine and Its Distinct Roles in the Bioenergetics of Trypanosoma cruzi, mSphere, 3 (2018).

[9] C.C. Avila, S.N. Mule, L. Rosa-Fernandes, R. Viner, M.J. Barison, A.G. Costa-Martins, G.S. Oliveira, M.M.G. Teixeira, C.R.F. Marinho, A.M. Silber, G. Palmisano, Proteome-Wide Analysis of Trypanosoma cruzi Exponential and Stationary Growth Phases Reveals a Subcellular Compartment-Specific Regulation, Genes (Basel), 9 (2018).

[10] M.J. Barisón, L.N. Rapado, E.F. Merino, E.M.F. Pral, B.S. Mantilla, L. Marchese, C. Nowicki, A.M. Silber, M.B. Cassera, Metabolomics profiling reveals a finely tuned, starvation-induced metabolic switch in Trypanosoma cruzi epimastigotes, J. Biol. Chem., (2017).

[11] L.S. Paes, B. Suárez Mantilla, F.M. Zimbres, E.M.F. Pral, P. Diogo de Melo, E.B. Tahara, A.J. Kowaltowski, M.C. Elias, A.M. Silber, Proline Dehydrogenase Regulates Redox State and Respiratory Metabolism in Trypanosoma cruzi, PLOS ONE, 8 (2013) e69419.

[12] M.J. Barison, F.S. Damasceno, B.S. Mantilla, A.M. Silber, The active transport of histidine and its role in ATP production in Trypanosoma cruzi, J. Bioenerg. Biomembr., 48 (2016) 437-449.

[13] B.S. Mantilla, L.S. Paes, E.M.F. Pral, D.E. Martil, O.H. Thiemann, P. Fernández-Silva, E.L. Bastos, A.M. Silber, Role of Δ1-Pyrroline-5-Carboxylate Dehydrogenase Supports Mitochondrial Metabolism and Host-Cell Invasion of Trypanosoma cruzi, J. Biol. Chem., 290 (2015) 7767-7790.

[14] D. Sylvester, S.M. Krassner, Proline metabolism in Trypanosoma cruzi epimastigotes, Comp. Biochem. Physiol. B: Biochem. Mol. Biol., 55 (1976) 443-447.

[15] R.M. Martins, C. Covarrubias, R.G. Rojas, A.M. Silber, N. Yoshida, Use of L-proline and ATP production by Trypanosoma cruzi metacyclic forms as requirements for host cell invasion, Infect. Immun., 77 (2009) 3023-3032.

[16] A.M. Silber, W. Colli, H. Ulrich, M.J. Alves, C.A. Pereira, Amino acid metabolic routes in Trypanosoma cruzi: possible therapeutic targets against Chagas' disease, Curr. Drug Targets Infect. Disord., 5 (2005) 53-64.

[17] P. Rohloff, C.O. Rodrigues, R. Docampo, Regulatory volume decrease in Trypanosoma cruzi involves amino acid efflux and changes in intracellular calcium, Mol. Biochem. Parasitol., 126 (2003) 219-230.

[18] A.-J.T. Contreras VT, Bonaldo MC, Thomaz N, Barbosa HS, Meirelles Mde N, Goldenberg S., Biological aspects of the Dm 28c clone of Trypanosoma cruzi after metacyclogenesis in chemically defined media., Mem Inst Oswaldo Cruz. , 83 (1988) 123-133.

[19] R.R. Tonelli, A.M. Silber, M. Almeida-de-Faria, I.Y. Hirata, W. Colli, M.J. Alves, L-proline is essential for the intracellular differentiation of Trypanosoma cruzi, Cell. Microbiol., 6 (2004) 733-741.

[20] A.M. Silber, R.R. Tonelli, C.G. Lopes, N. Cunha-e-Silva, A.C.T. Torrecilhas, R.I. Schumacher, W. Colli, M.J.M. Alves, Glucose uptake in the mammalian stages of Trypanosoma cruzi, Mol. Biochem. Parasitol., 168 (2009) 102-108.

[21] A. Magdaleno, I.Y. Ahn, L.S. Paes, A.M. Silber, Actions of a proline analogue, L-thiazolidine-4-carboxylic acid (T4C), on Trypanosoma cruzi, PLoS One, 4 (2009) e4534.

[22] M. Sayé, M.R. Miranda, F. di Girolamo, M. de los Milagros Cámara, C.A. Pereira, Proline Modulates the Trypanosoma cruzi Resistance to Reactive Oxygen Species and Drugs through a Novel D, L-Proline Transporter, PLOS ONE, 9 (2014) e92028.

[23] B.S. Mantilla, L. Marchese, A. Casas-Sánchez, N.A. Dyer, N. Ejeh, M. Biran, F. Bringaud, M.J. Lehane, A. Acosta-Serrano, A.M. Silber, Proline Metabolism is Essential for Trypanosoma brucei brucei Survival in the Tsetse Vector, PLoS Path., 13 (2017) e1006158.

[24] A.M. Silber, R.R. Tonelli, M. Martinelli, W. Colli, M.J. Alves, Active transport of L-proline in Trypanosoma cruzi, J. Eukaryot. Microbiol., 49 (2002) 441-446.

[25] T. Heinrich, H. Böttcher, R. Gericke, G.D. Bartoszyk, S. Anzali, C.A. Seyfried, H.E. Greiner, C. van Amsterdam, Synthesis and Structure−Activity Relationship in a Class of Indolebutylpiperazines as Dual 5-HT1A Receptor Agonists and Serotonin Reuptake Inhibitors, J. Med. Chem., 47 (2004) 4684-4692.

[26] R. Xue, Z.-L. Jin, H.-X. Chen, L. Yuan, X.-H. He, Y.-P. Zhang, Y.-G. Meng, J.-P. Xu, J.-Q. Zheng, B.-H. Zhong, Y.-F. Li, Y.-Z. Zhang, Antidepressant-like effects of 071031B, a novel serotonin and norepinephrine reuptake inhibitor, Eur. Neuropsychoph., 23 (2013) 728-741.

[27] S.B. Vogensen, L. Jørgensen, K.K. Madsen, N. Borkar, P. Wellendorph, J. Skovgaard-Petersen, A. Schousboe, H.S. White, P. Krogsgaard-Larsen, R.P. Clausen, Selective mGAT2 (BGT-1) GABA Uptake Inhibitors: Design, Synthesis, and Pharmacological Characterization, J. Med. Chem., 56 (2013) 2160-2164.

[28] M.L. López-Rodríguez, A. Viso, S. Ortega-Gutiérrez, I. Lastres-Becker, S. González, J. Fernández-Ruiz, J.A. Ramos, Design, Synthesis and Biological Evaluation of Novel Arachidonic Acid Derivatives as Highly Potent and Selective Endocannabinoid Transporter Inhibitors, J. Med. Chem., 44 (2001) 4505-4508.

[29] M.L. López-Rodríguez, A. Viso, S. Ortega-Gutiérrez, C.J. Fowler, G. Tiger, E. de Lago, J. Fernández-Ruiz, J.A. Ramos, Design, Synthesis, and Biological Evaluation of New

Inhibitors of the Endocannabinoid Uptake: Comparison with Effects on Fatty Acid Amidohydrolase, J. Med. Chem., 46 (2003) 1512-1522.

[30] J.W. Clader, The discovery of ezetimibe: a view from outside the receptor, J. Med. Chem., 47 (2004) 1-9.

[31] J.L. Betters, L. Yu, NPC1L1 and cholesterol transport, FEBS Lett., 584 (2010) 2740-2747.

[32] K. Hashimoto, Glycine Transport Inhibitors for the Treatment of Schizophrenia, Open Med. Chem. J., 4 (2010) 10-19.

[33] J.E. Carland, C.A. Handford, R.M. Ryan, R.J. Vandenberg, Lipid inhibitors of high affinity glycine transporters: Identification of a novel class of analgesics, Neurochem. Int., 73 (2014) 211-216.

[34] E. Pinard, A. Alanine, D. Alberati, M. Bender, E. Borroni, P. Bourdeaux, V. Brom, S. Burner, H. Fischer, D. Hainzl, R. Halm, N. Hauser, S. Jolidon, J. Lengyel, H.-P. Marty, T. Meyer, J.-L. Moreau, R. Mory, R. Narquizian, M. Nettekoven, R.D. Norcross, B. Puellmann, P. Schmid, S. Schmitt, H. Stalder, R. Wermuth, J.G. Wettstein, D. Zimmerli, Selective GlyT1 Inhibitors: Discovery of [4-(3-Fluoro-5-trifluoromethylpyridin-2-yl)piperazin-1-yl][5-methanesulfonyl-2-((S)-2,2,2-trifluoro-1-methylethoxy)phenyl]methanone (RG1678), a Promising Novel Medicine To Treat Schizophrenia, J. Med. Chem., 53 (2010) 4603-4614.

[35] M. Hauptmann, D.F. Wilson, M. Erecińska, High affinity proline uptake in rat brain synaptosomes, FEBS Lett., 161 (1983) 301-305.

[36] X.-C. Yu, W. Zhang, A. Oldham, E. Buxton, S. Patel, N. Nghi, D. Tran, T.H. Lanthorn, C. Bomont, Z.-C. Shi, Q. Liu, Discovery and characterization of potent small

molecule inhibitors of the high affinity proline transporter, Neurosci. Lett., 451 (2009) 212-216.

[37] M.R. Burns, G.F. Graminski, R.S. Weeks, Y. Chen, T.G. O'Brien, Lipophilic Lysine−Spermine Conjugates Are Potent Polyamine Transport Inhibitors for Use in Combination with a Polyamine Biosynthesis Inhibitor, J. Med. Chem., 52 (2009) 1983-1993.

[38] S.G. Agalave, S.R. Maujan, V.S. Pore, Click Chemistry: 1,2,3-Triazoles as Pharmacophores, Chem. Asian J., 6 (2011) 2696-2718.

[39] G.C. Tron, T. Pirali, R.A. Billington, P.L. Canonico, G. Sorba, A.A. Genazzani, Click chemistry reactions in medicinal chemistry: applications of the 1,3-dipolar cycloaddition between azides and alkynes, Med. Res. Rev., 28 (2008) 278-308.

[40] E.O. Porta, P.B. Carvalho, M.A. Avery, B.L. Tekwani, G.R. Labadie, Click chemistry decoration of amino sterols as promising strategy to developed new leishmanicidal drugs, Steroids, 79 (2014) 28-36.

[41] A.R. Hamann, C. de Kock, P.J. Smith, W.A. van Otterlo, M.A. Blackie, Synthesis of novel triazole-linked mefloquine derivatives: biological evaluation against Plasmodium falciparum, Bioorg. Med. Chem. Lett., 24 (2014) 5466-5469.

[42] I. Carvalho, P. Andrade, V.L. Campo, P.M. Guedes, R. Sesti-Costa, J.S. Silva, S. Schenkman, S. Dedola, L. Hill, M. Rejzek, S.A. Nepogodiev, R.A. Field, 'Click chemistry' synthesis of a library of 1,2,3-triazole-substituted galactose derivatives and their evaluation against Trypanosoma cruzi and its cell surface trans-sialidase, Bioorg. Med. Chem., 18 (2010) 2412-2427.

[43] C. Gauchet, G.R. Labadie, C.D. Poulter, Regio- and chemoselective covalent immobilization of proteins through unnatural amino acids, J. Am. Chem. Soc., 128 (2006) 9274-9275.

[44] Craig S. McKay, M.G. Finn, Click Chemistry in Complex Mixtures: Bioorthogonal Bioconjugation, Chem. Biol., 21 (2014) 1075-1101.

[45] R.N. Hannoush, J. Sun, acylation and prenylation, Nat. Chem. Biol., 6 (2010) 498-506.

[46] A.S. Thompson, G.R. Humphrey, A.M. DeMarco, D.J. Mathre, E.J.J. Grabowski, Direct conversion of activated alcohols to azides using diphenyl phosphorazidate. A practical alternative to Mitsunobu conditions, J. Org. Chem., 58 (1993) 5886-5888.

[47] A. Gagneuz, S. Winstein, W.G. Young, Rearrangement of allyl azides, J. Org. Chem., 1 (1969) 5956-5957.

[48] E.O.J. Porta, M.M. Vallejos, A.B.J. Bracca, G.R. Labadie, Experimental and theoretical studies of the [3,3]-sigmatropic rearrangement of prenyl azides, RSC Adv., 7 (2017) 47527-47538.

[49] V.V. Rostovtsev, L.G. Green, V.V. Fokin, K.B. Sharpless, A stepwise huisgen cycloaddition process: copper(I)-catalyzed regioselective "ligation" of azides and terminal alkynes, Angew. Chem., 41 (2002) 2596-2599.

[50] G.R. Labadie, A. de la Iglesia, H.R. Morbidoni, Targeting tuberculosis through a small focused library of 1,2,3-triazoles, Mol. Divers., 15 (2011) 1017-1024.

[51] E.O.J. Porta, S.N. Jäger, I. Nocito, G.I. Lepesheva, E.C. Serra, B.L. Tekwani, G.R. Labadie, Antitrypanosomal and antileishmanial activity of prenyl-1,2,3-triazoles, MedChemComm, 8 (2017) 1015-1021.

[52] Z. Brener, E. Chiari, Aspects of early growth of different Trypanosoma cruzi strains in culture medium, J. Parasitol., 51 (1965) 922-926.

[53] F.S. Damasceno, M.J. Barisón, E.M.F. Pral, L.S. Paes, A.M. Silber, Memantine, an Antagonist of the NMDA Glutamate Receptor, Affects Cell Proliferation, Differentiation and the Intracellular Cycle and Induces Apoptosis in Trypanosoma cruzi, PLOS Neglected Tropical Diseases, 8 (2014) e2717.

[54] M. Sayé, L. Fargnoli, C. Reigada, G.R. Labadie, C.A. Pereira, Evaluation of proline analogs as trypanocidal agents through the inhibition of a Trypanosoma cruzi proline transporter, Biochimica et Biophysica Acta (BBA) - General Subjects, 1861 (2017) 2913-2921.

[55] N.G. Norager, C.B. Jensen, M. Rathje, J. Andersen, K.L. Madsen, A.S. Kristensen, K. Stromgaard, Development of Potent Fluorescent Polyamine Toxins and Application in Labeling of Ionotropic Glutamate Receptors in Hippocampal Neurons, ACS Chem Biol, (2013).

[56] D.M.C. Ramirez, W.W. Ogilvie, L.J. Johnston, NBD-cholesterol probes to track cholesterol distribution in model membranes, Biochim. Biophys. Acta, 1798 (2010) 558-568.

[57] M.A. Kol, A. van Dalen, A.I.P.M. de Kroon, B. de Kruijff, Translocation of Phospholipids Is Facilitated by a Subset of Membrane-spanning Proteins of the Bacterial Cytoplasmic Membrane, J. Biol. Chem., 278 (2003) 24586-24593.

[58] J. Pohl, A. Ring, W. Stremmel, Uptake of long-chain fatty acids in HepG2 cells involves caveolae: analysis of a novel pathway, J. Lipid Res., 43 (2002) 1390-1399.

[59] J.G. Woodland, R. Hunter, P.J. Smith, T.J. Egan, Shining new light on ancient drugs: preparation and subcellular localisation of novel fluorescent analogues of Cinchona alkaloids in intraerythrocytic Plasmodium falciparum, Organic & Biomolecular Chemistry, 15 (2017) 589-597.

[60] http://www.molinspiration.com. v2014.11, 20-08-2015., in.

[61] K. Suthagar, A.J. Fairbanks, A new way to do an old reaction: highly efficient reduction of organic azides by sodium iodide in the presence of acidic ion exchange resin, Chem. Commun., 53 (2017) 713-715.

[62] A.W. Schwabacher, J.W. Lane, M.W. Schiesher, K.M. Leigh, C.W. Johnson, Desymmetrization reactions: efficient preparation of unsymmetrically substituted linker molecules, The Journal of Organic Chemistry, 63 (1998) 1727-1729.

[63] Y. Guminski, M. Grousseaud, S. Cugnasse, V. Brel, J.-P. Annereau, S. Vispé, N. Guilbaud, J.-M. Barret, C. Bailly, T. Imbert, Synthesis of conjugated spermine derivatives with 7-nitrobenzoxadiazole (NBD), rhodamine and bodipy as new fluorescent probes for the polyamine transport system, Bioorg. Med. Chem. Lett., 19 (2009) 2474-2477.

[64] See supporting information

[65] M.L. Merli, L. Pagura, J. Hernández, M.J. Barisón, E.M.F. Pral, A.M. Silber, J.A. Cricco, The Trypanosoma cruzi Protein TcHTE Is Critical for Heme Uptake, PLOS Neglected Tropical Diseases, 10 (2016) e0004359.

[66] J.M. Saugar, J. Delgado, V. Hornillos, J.R. Luque-Ortega, F. Amat-Guerri, A.U. Acuña, L. Rivas, Synthesis and Biological Evaluation of Fluorescent Leishmanicidal Analogues of Hexadecylphosphocholine (Miltefosine) as Probes of Antiparasite Mechanisms, J. Med. Chem., 50 (2007) 5994-6003.

[67] U. Eckstein-Ludwig, R.J. Webb, I.D.A. van Goethem, J.M. East, A.G. Lee, M. Kimura, P.M. O'Neill, P.G. Bray, S.A. Ward, S. Krishna, Artemisinins target the SERCA of Plasmodium falciparum, Nature, 424 (2003) 957.

[68] J.G. Woodland, R. Hunter, P.J. Smith, T.J. Egan, Chemical Proteomics and Super-resolution Imaging Reveal That Chloroquine Interacts with Plasmodium falciparum

Multidrug Resistance-Associated Protein and Lipids, ACS Chemical Biology, 13 (2018) 2939-2948.

[69] Z. Brener, E. Chiari, Aspects of early growth of different Trypanosoma cruzi strains in culture medium, J. Parasitol., 51 (1965) 922-926.

[70] E. Camargo, Growth and Differentiation in Trypanosoma cruzi-I. Origin of Metacyclic Trypanosomes in Liquid Media, Rev. Jnst. Med. Trop. Sao Paulo, 6 (1964) 93-100.

[71] W.S. Rasband, ImageJ, , U. S. National Institutes of Health, Bethesda, Maryland, USA.

[72] C.A. Schneider, W.S. Rasband, K.W. Eliceiri, NIH Image to ImageJ: 25 years of image analysis, Nat. Methods, 9 (2012) 671.

Graphical Abstract

Leave this area blank for abstract info.

Rationally design of a proline transporter inhibitor with anti-*Trypanosoma cruzi* activity.

Lucía Fargnoli, Esteban A. Panozzo-Zénere, Lucas Pagura, María Julia Barisón, Julia A. Cricco, Ariel M. Silber and Guillermo R. Labadie*